ANALYSIS OF THE SMALL GTP BINDING PROTEIN RAC2

by

Meagan Alyssa Snodgrass

A thesis submitted in partial fulfillment
of the requirements for the degree

of

Master of Science

in

Microbiology

MONTANA STATE UNIVERSITY
Bozeman, Montana

May 2005

APPROVAL

of a thesis submitted by

Meagan Alyssa Snodgrass

This thesis has been read by each member of the thesis committee and has been found to be satisfactory regarding content, English usage, format, citations, bibliographic style, and consistency, and is ready for submission to the College of Graduate Studies.

Dr. Algirdas J. Jesaitis

Approved for the Department of Microbiology

Dr. Tim Ford

Approved for the College of Graduate Studies

Dr. Bruce McLeod

STATEMENT OF PERMISSION TO USE

In presenting this thesis in partial fulfillment of the requirements for a master's degree at Montana State University, I agree that the Library shall make it available to borrowers under rules of the Library.

If I have indicated my intention to copyright this thesis by including a copyright notice page, copying is allowable only for scholarly purposes, consistent with "fair use" as prescribed in the U.S. Copyright Law. Requests for permission for extended quotation from or reproduction of this thesis in whole or in parts may be granted only by the copyright holder.

Meagan Alyssa Snodgrass

May 5, 2005

TABLE OF CONTENTS

TABLE OF CONTENTS - CONTINUED

LIST OF TABLES

Table Page

LIST OF FIGURES

LIST OF FIGURES - CONTINUED

Figure Page

ABSTRACT

Human neutrophils serve as the first line of immune defense against invading pathogens. In many cells, including neutrophils, Rac proteins are key regulators of many diverse cellular functions through their affects on cytoskeletal organization and in neutrophils, the NADPH oxidase complex, a critical mechanism for host defense. The primary purpose of this research is to examine the possibility that Rac2 interacts directly with the actin cytoskeleton. A different small GTP binding protein, Rap2 has been shown to interact with actin through direct binding.

To test our hypothesis, GST-Rac2 and GST-Rac2 R120E protein was expressed in *E. coli.* Rac2 was then purified and used for phage display mapping to identify potential binding epitopes on actin. Phage display analysis, which has been used to map binding epitopes on other proteins, was conducted on GST-Rac2 and GST-Rac2 R120E affinity columns. Peptide sequences from phage display on both proteins were mapped to the amino acid sequence of human actin using the program FINDMAP. This program can identify discontinuous epitope regions by permitting large gaps in the target sequence during alignment. FINDMAP results were visualized using Swiss PDB Viewer, a publicly available protein modeling program and workbench. Several possible binding epitopes for Rac2 were identified on the surface of actin.

Purified GST-Rac2 was shown to bind GTPγ [^{35}S] selectively, but GST-Rac2 R120E did not bind GTPγ [^{35}S]. Fluorescence spectroscopy results suggested that the structural conformation of the purified wild type and mutant protein were similar. Protein characterization shows that while only GST-Rac2 can bind nucleotide, both proteins are structurally similar.

In addition to the purification of recombinant protein expressed in *E. coli*, we generated vectors to express c-myc tagged Rac2 and Rac2 R120E in mammalian cell lines. Preliminary fluorescence microscopy data shows that indeed c-myc tagged Rac2 and Rac2 R120E are expressed using an inducible transfection system. Future studies will determine the effect of Rac2 R120 E on the actin cytoskeleton in mammalian cells.

Taken with previous data suggesting that Rac2 and Rac2 R120E binds actin, this research strengthens the argument that Rac2 and actin interact in a direct manner.

CHAPTER 1

INTRODUCTION

Overview of Neutrophil Cell Biology

Innate immunity is the first line of defense against invading pathogens (Smith, 1994). Phagocytes are a central component of the innate immune system and employ a variety of mechanisms to prevent growth and proliferation of infectious agents. The basic process used by phagocytes to attack invaders is called phagocytosis. During phagocytosis, bacteria and foreign particles that gain entry into the body are engulfed, injured, digested, and destroyed. Not only do phagocytes destroy invading bacteria, but they also alert the adaptive immune response to the presence of infection, making the phagocyte response critical for maintaining health.

The main population of phagocytic cells in the body is the short-lived neutrophils, also known as polymorphonuclear leukocytes (PMNs). These cells account for 55-75% of the total leukocyte population. There are 2-4 x 10^3 neutrophils/μl in peripheral blood of adults, and 10^9 cells/kg/day are made in the bone marrow (Smith, 1994). The production of neutrophils is increased up to ten-fold in response to infection. Neutrophils have a distinct morphology with a multi-lobed nucleus and a large number of cytoplasmic granules. Neutrophils reside in the blood for approximately 4-10 hours, after which they migrate to tissue, and it is believed that they survive for 1-2 days before undergoing apoptosis .

Neutrophils Protect Against Infection

Neutrophils circulate in the bloodstream and maintain surveillance for signs of infection, injury, or foreign substances. When neutrophils detect bacteria, they adhere and transmigrate through the endothelium out of the bloodstream and into the effected tissue. Neutrophils recognize chemoattractant signals released by pathogens and generate directed movement or chemotaxis to reach the invading organism. In a well orchestrated procedure, bacteria are bound by a long membrane extensions or lamellipodium that wrap around and engulf bacteria into the neutrophil. Once internalized, bacteria are destroyed by toxic components contained or produced within neutrophils. The chemical armory of neutrophils includes molecules such as highly toxic reactive oxygen species (ROS), hydrolytic proteins, and cationic peptides which disable bacteria (Lee, 2003). Under appropriate conditions, bacteria are destroyed within a membrane bound phagolysosome, thus minimizing exposure of inflammatory compounds to normal host tissue. Neutrophils employ protective mechanisms that reduce self-induced oxidative damage such as superoxide dismutatse, catalase and the hexose monophosphage shunt enzymes (Werner, 2004). Nevertheless, unchecked or inappropriate neutrophil activation causes inflammation that may lead to a plethora of disease states. The defensive molecules generated by activated neutrophils are toxic to both pathogens and host tissue. Therefore, activation is tightly regulated which ensures that neutrophils function properly to defend the host without causing excess tissue damage. Understanding the complex molecular biology of neutrophils may, in time, allow the rational design of compounds to augment host defenses with mitigated consequences for healthy host tissues.

Neutrophil Activation

Infectious microorganisms release small molecules that disperse in a gradient around an infected area and alert the immune system to their presence. Part of this alert system is the generation of inflammation and inflammatory mediators. The first cells to respond to such infections are neutrophils. Neutrophils reside in the bloodstream and when microorganism products or mediators of inflammation disperse around an area of inflammation, neutrophils bind and flatten on the endothelial surface of nearby blood vessels and migrate through the vessels towards the pathogen (Burg, 2001). Neutrophils are activated by many agents including: 1) bacterial products such as the small peptide formylated-Met-Leu-Phe (fMLF); 2) products of lipid metabolism that are released from activated platelets, endothelial cells, and leukocytes; 3) activated complement factors; and 4) other serum factors such as immune complexes. These regulatory molecules bind to receptors on the surface of the neutrophil, and provide the signals for the cells migration and activation (Jesaitis, 1988). In this activated state, neutrophils are primed to destroy pathogens. However, if neutrophils become activated in response to host tissue, pathogenic conditions such as vascular inflammation or arthritis may result. Neutrophils activated in a more systemic fashion may mediate severe shock leading to massive vascular leakage and even death.

Chemotaxis and Transendothelial Migration

Neutrophil chemotaxis depends on the recognition of a concentration gradient of a chemoattractant by extracellular receptors which cause the cell to become polarized. The polarization results from both the formation of a leading lamellipodium, that moves

towards the chemoattractant source and a retracting tail called a uropod. The mechanism by which cells generate forward movement involves intricate control of the cellular cytoskeleton and membrane remodeling to coordinate cellular extension and contraction in a process reminiscent of crawling. Multicellular organisms depend on the chemotactic abilities of immune cells such as neutrophils to defend against infection and evolution has buttressed the ability of these cells to function correctly by creating multiple signals to insure appropriate directed migration (Van Haastert, 2004).

Following activation by inflammatory stimuli, neutrophils are the first immune cells to bind to the activated endothelium and migrate through the tissue to the infected area in a process known as extravasation. There are four well-characterized steps in neutrophil extravasation including capture, rolling, adhesion, and transendothelial migration. Normally, cells move along the vasculature by flow or by rolling along the endothelium. Upon activation by chemoattractant stimuli, neutrophils arrest and spread and adhere tightly before engaging in transendothelial migration (Blankenberg, 2003.). During rolling, neutrophils tether to the endothelium via weak carbohydrate-selectin interactions, but are swept away by shear force caused by normal blood circulation. This interaction occurs with numerous endothelial cells causing the neutrophil to slow. While the neutrophil is rolling, it can be activated through exposure to chemoattractants including chemokines, platelet activating factor (PAF), and N-formyl peptides produced by bacteria. Ligation of receptors on the surface of neutrophils, especially the seven transmembrane domain G protein receptors, initiates signal transduction pathways that lead to a conformational change in integrin proteins expressed on the neutrophil surface

(Worthylake, 2001). Such conformational changes allow the integrin molecules to adhere tightly to Ig-superfamily cell adhesion molecules (CAM) expressed on activated endothelial cells, stabilizing neutrophil adhesion to the endothelium. Several cellular mechanisms likely exist to allow neutrophil transport across and through endothelial barriers during microbial or inflammatory insult. Inflammatory molecules may induce local epithelial cells to relax contacts at epithelial junctions (Johnson-Leger, 2003) which would increase permeability of this otherwise tight barrier, facilitating extravasation and tissue transmigration.

Introduction to Rac

Rac2 Influences Neutrophil Functions

One of the global regulators of neutrophil functions, be it activation, chemotaxis, phagocytosis, transendothelial migration, degranulation, or NADPH oxidase activity is the Rho family of GTP binding proteins. The following sections serve to describe the molecular properties of the small G-protein Rac2 and the role that Rac2 plays in a diverse array of cellular functions. Rac2 regulates many cellular functions by causing the rearrangement of the actin cytoskeleton. In the absence Rac2 expression, human neutrophils are unable to function properly, resulting in chronic infection due to immune deficiency. Although neutrophil biology will be emphasized here, there have been many recent publications describing Rac function in a variety of other cell types including neurons, fibroblasts, *Dictyostelium* and yeast (VanHaastert 2004). Despite over a decade

of research on the role of Rac in cellular function, the precise signaling pathways that enable Rac to interact with the cell cytoskeleton have yet to be fully elucidated.

Rho GTPase Structure and Function

Rac is one of twenty mammalian proteins in the Rho family of small GTP-binding proteins. Initial interest in the Rho family of GTPases began when they were identified as cousins of the oncogenic Ras proteins. Each of the Rho (Ras homology) family proteins contributes to the formation of cytoskeletal protrusions and contractions. The Rho family of proteins, Rho, Rac and Cdc42, share around 50-60% amino acid identity between them and have about 30% identity to the Ras proteins (Foster, 1996).

The Rac proteins are key regulators of many diverse cellular functions through their effects on cytoskeletal organization. In different cellular locations, Rac activates pathways in many tissues including actin remodeling, motility, gene expression, and cell cycle progression (Freeman, 1994). B cell proliferation and survival (Gu, 2003), T cell receptor-activated proliferation, and T cell cytokine generation (Tybulewicz, 2003) also require Rac. Rac has also been shown to cause tumorigenesis due to mutations (Gao, 2004).

Several isoforms of Rac (Rac 1, 2, and 3) have been identified to date. Rac1 and 3 are ubiquitously expressed while Rac2 is the physiological Rac found in hematopoietic cells. Rac2 is the major isoform in human neutrophils and is critical for the generation of reactive oxygen species by the NADPH oxidase complex (Filippi, 2004). The Rac isoforms have 92% amino acid sequence identity, differing mainly in the C-terminus. It serves to note that many of the model systems discussed in the following sections have

used Rac1 instead of Rac2. In phagocytes, Rac1 is effective in generating ROS in the oxidase system, although *in vivo*, Rac2 localizes to the membrane more efficiently than Rac1. Ninety two percent of the Rac expressed by human neutrophils is Rac2, but murine neutrophils have about a 50:50 ratio of Rac1 to Rac2 (Li, 2002).

Rho Proteins Act as Molecular Switches

Rac2 acts as a molecular switch to activate cytoskeletal rearrangement and neutrophil function. Rac2 is activated only when bound to GTP and remains inactive when bound to GDP. Paradoxically, the same cytotoxic compounds that allow neutrophils to fend off invaders during an infection can cause disease if they are activated in error. To prevent host tissue damage, Rac2 and other small GTP binding proteins are tightly regulated to ensure they only bind GTP and become activated under appropriate conditions. The tightly regulated mechanism of the GTP-activated molecular switch is shown in Figure 1. Three main groups of proteins regulate the function of Rac2: 1) guanine-nucleotide exchange factors (GEF), which catalyze release of GDP and binding of GTP; 2) GTPase activators (GAPs), which speed up the hydrolysis of GTP by small G proteins; and 3) guanine dissociation inhibitors (GDI), which inhibit nucleotide exchange.

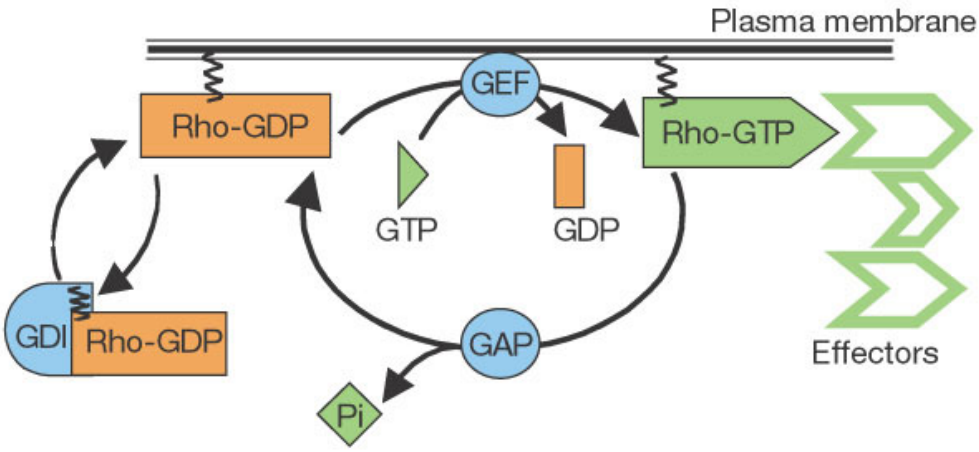

Figure 1. The Rho GTPase Cycle. The Rho GTPases cycle between an active, GTP bound, and an inactive GDP bound conformation. The cycle is tightly regulated in mammals by the guanine nucleotide exchange factors (GEFs), guanine activating proteins (GAPs) and guanine nucleotide exchange inhibitors (GDIs). All Rho GTPases are prenylated at their C-terminus for proper membrane localization.
(figure from Etienne-Manneville and Hall, 2002)

Cellular Processes driven by Rho, Rac, and Cdc42 activation

Rho, Rac and Cdc42 are the small G proteins involved in transendothelial migration, neutrophil orientation, and chemotaxis in response to inflammatory stimuli. They are triggers of directed actin polymerization resulting in a variety of cellular structures that facilitate the above processes (Katanaev, 2001). Wound healing assays have shown that inhibition of the Rho GTPases results in failure of the following cellular processes: "(i) polymerization of actin to form filaments, (ii) formation of lamellipodia, filopodia and stress fibers, (iii) cell motility, (iv) cell spreading and (v) cell-to-cell adhesions" (Begum, 2004). The NIH 3T3 cells used in the Begum experiments were inactivated through induced expression of a Rho GAP, which bound to Rho, Rac, and Cdc42 and prevented the proteins from functioning in a proper cell response.

Distinct, but interrelated roles for the Rho family GTPases in neutrophils and other cells have been reported. The Rho family proteins are all involved in regulating cytoskeletal organization. The structures caused by Rac activation include membrane ruffles and lamellipodia. Cdc42 can also cause the formation of membrane ruffles and lamellipodia, but through a different activation pathway (Cox, 1997). Lamellipodia are narrow protrusions reaching out from the leading edge of a migrating cell, and are generated by cytoskeletal rearrangement. Filamentous actin has been isolated in lamellipodia along with other proteins including integrins, vinculin and paxillin (Schmidt, 1998). Membrane ruffles form when lamellipodia fail to adhere to the surface, but also occur at the dorsal edge of migrating and non-migrating cells. The exact function of membrane ruffles is not known, but the structures mediate accumulation of large vesicles of material from the extracellular environment (Ridley, 1992.), so they may be involved in sampling of the environment and pinocytosis. Cdc42 regulates filopodia formation and plays a role in chemotaxis. Rho promotes the formation of actin stress fibers and focal adhesions (Chimini, 2000).

Rho and Rac induce integrin clustering and focal adhesions. Disrupting Rho or Rac function in cells results in a rounded phenotype and causes the loss of adhesion. The reason for decreased attachment may reflect a collapse of cellular actin organization and polymerization. Cells that do not express Rac exhibit a similar phenotype to cells treated with drugs that cause actin depolymerization, which illustrates the critical role Rac plays in regulating actin (Burridge, 2004).

Phagocytosis in response to an immunoglobulin (Type 1) is mediated by Rac and Cdc42, while complement mediated phagocytosis (Type 2) is controlled by Rho (Caron, 1998). Rac activation has been shown to cause rapid actin polymerization leading to membrane extensions, while Rho activation caused existing actin filaments to become bundled leading to stress fibers (Machesky, 1997). Interestingly, Rho and Rac were shown to influence endothelial cell permeability resulting in transendothelial migration (Wojciak-Stothard, 2001). Membrane extensions contain adhesive structures including focal complexes and podosomes to pull them forward. The rear of the cell releases the subsurface and retracts through Rho A signaling pathways causing the depolymerization of actin (Worthylake, 1991).

Unique Rac2 Structural Features

The main amino acid sequence difference between Rac1 and Rac2 occurs near the C-terminal prenylation consensus site (CAAX box). In Rac1, this sequence is 183-KKRKRK, a strongly polybasic motif, but in Rac2 the sequence in this region is 183-RQQKRP, replacing three of the charged amino acids (K and R) with the neutral amino acids Q and P. In cells treated with FMLF, both the RQQKRP motif and D150 were critical for actin polymerization and chemotaxis. Filippi et al mutated the Rac2 CAAX to 183-KKRKRK (the Rac1 sequence in this region) and the resulting murine neutrophils failed to produce superoxide. The C-terminal CAAX box is likely responsible for the localization of the protein *in vivo* and mutations to this region effects post-translational modifications associated with this region of Rac preventing proper protein function (Filippi, 2004). Differences in function between Rac isoforms have been characterized in

mice deficient in Rac2 and show that Rac2 has unique functions in neutrophils that cannot be performed by Rac1. Loss of Rac2 activity has been associated with a loss of chemotaxis and superoxide production (Roberts, 1999).

Rac2 as a Molecular Compass

The method by which neutrophils orient themselves in their environment to migrate up a chemotactic gradient involves both spatial and temporal regulation. The cell must recognize the gradient to reorganize into a polarized morphology and must also sense a change in concentration over time at its leading edge to move in the correct direction. Migratory eukaryotic cells including neutrophils and *Dictyostelium discoideum* can respond to differences in chemotactic gradients as small as 2-10% between the front and rear of the cell (Van Haastert, 2004). One mechanism by which neutrophils navigate involves the regulation of cellular function by Rac1 and Rac2. It has been shown that the specific roles of Rac1 and Rac2 in chemotaxis differ between murine neutrophils and human neutrophils. The authors of the former study used Cre recombinase to make mice deficient in either Rac1, Rac2 or both. The Rac1 deficient cells (expressing only Rac2) would migrate without orientation to the chemoattractant source, while the Rac2 null cells could generate lamellipodia facing the gradient but could not efficiently migrate (Sun, 2004). Further details concerning the role of Rho-family GTPases in actin polymerization will be outlined in a subsequent section.

A Human Rac2 Mutant Results in Serious Immune Deficiency

Several immunodeficiency syndromes exist when neutrophils fail to function properly. The best characterized neutrophil defects include chronic granulomatous disease (CGD), in which neutrophils fail to produce toxic oxygen products to neutralize infection (Roos, 2003) and leukocyte adhesion disorder (LAD) where neutrophils fail to adhere to endothelial surfaces and thus, cannot reach infected areas (Harlan, 1993). Advances in molecular biology have allowed researchers to pinpoint the cause of certain immunodeficiencies, leading to greater knowledge about the mechanics of the immune system.

A neutrophil defect was suspected in an infant male when he presented with multiple infections and was unable to heal wounds. Blood samples were examined and revealed that the patient had an elevated neutrophil count, but that these cells were unable to engage in chemotaxis, polarize, release the contents of azurophilic granules, or produce superoxide anions in response to a variety of activating stimuli. These neutrophils were found to express normal basal levels of CD11b, an adhesive molecule, which is inconsistent with the defect caused by LAD. The patient's neutrophils increased CD11b expression and released the contents of their secondary granules in response to activating factors at the same levels as control neutrophils from healthy adults, indicating that the neutrophils could recognize the presence of chemoattractant stimuli. CGD presents a similar defect in superoxide production, but does not interfere with chemotaxis or polarization, making this an unlikely diagnosis.

Western blot analysis revealed that Rac2, which is critical for both actin dynamics and the generation of superoxide, was expressed at much lower levels by the patient's neutrophils than in control neutrophils. Addition of recombinant Rac could restore superoxide production by isolated membranes from these cells. Genetic analysis showed that a mutation of one Rac2 allele led to the expression of only the defective protein Rac2 D57N. Mutational analysis on the related protein Ras shows that changing this aspartate residue inhibits exchange of GDP to GTP and prevents Ras signaling. Similar studies on other small GTP binding proteins have shown that mutant GTPases are structurally unstable, which may explain the reduced level of Rac2 detected in the patient's neutrophils. Also, the Rac2 D57N expressed by the patient was shown to inhibit superoxide production stimulated by wild-type GTP bound Rac, suggesting that while D57N Rac2 does not become activated, it can bind other components of the oxidase in a competitive manner. This analysis demonstrates that mutations in Rac2 can lead to neutrophil dysfunction resulting in severe immunodeficiencies.

Neutrophil Killing of Bacteria

As previously stated, neutrophils are the first line of defense against invading organisms. They migrate to sites of infection faster and in greater numbers than any other immune cell. Neutrophils phagocytize pathogens and destroy them by two separate, but intertwined processes: oxidative and non-oxidative killing. Additionally, novel mechanisms for neutrophil defensive strategies are still being uncovered. The

following sections describe neutrophil killing mechanisms in greater molecular detail and, where applicable, highlight known roles of Rac in these processes.

Generation of Reactive Oxygen Species by the NADPH Oxidase Complex

Oxidative killing by neutrophils is achieved through the generation of reactive oxygen species (ROS). These toxic metabolites are produced through the reduction of molecular oxygen (O_2) into the reactive precursor species superoxide anion (O_2^-) during the respiratory burst, a reaction that is mediated through the activation of the NADPH oxidase. Additional reactive oxygen species are derived from superoxide and include hydroxyl radical, hydrogen peroxide, hypochlorite, peroxynitrite, ozone, and related products.

The NADPH oxidase pathway is critical for host defense. Chronic granulomatous disease results from dysfunction or absence of any of a number of components in the NADPH oxidase complex. The resulting pathology from these genetic defects includes chronic bacterial and fungal infections. Persistent activation of NADPH oxidase leads to inflammatory disease such as arthritis, due to uncontrolled production of reactive oxygen species.

In addition to the killing function of ROS, these oxygen products have recently been identified as crucial signaling molecules in a wide variety of tissues. For example, the vascular system appears to be influenced by ROS, and the pathology of inflammation involved in atherosclerosis has been highly correlated with the expression of the NADPH oxidase in macrophages, which produce oxygen radicals around plaque formations in coronary artery disease (Sorescu, 2002).

Structure of the NADPH Oxidase Complex

Because of the importance of the NADPH oxidase in immunity and the implications of unchecked inflammation, mechanistic aspects of this large, multi-subunit complex have been extensively studied. There are six components to the NADPH oxidase, two transmembrane proteins ($gp91^{phox}$ and $p22^{phox}$) which together form flavocytochrome b_{558} and four cytosolic subunits, ($p47^{phox}$, $p67^{phox}$, Rac2 and $p40^{phox}$) which translocate to the plasma membrane after neutrophil activation.

The membrane bound component of the NADPH oxidase is flavocytochrome b_{558}, a heterodimeric, integral membrane protein composed of $gp91^{phox}$ and $p22^{phox}$ subunits. The larger subunit, $gp91^{phox}$, is predicted to coordinate two heme prosthetic groups, the NADPH binding site, and bound flavin adenine dinucleotide (FAD). When the oxidase is assembled at the membrane, it acts as a scaffold to facilitate transfer of electrons by a multi-step process. First, an electron is transferred from NADPH to FAD in the cytosolic domain of flavocytochrome b_{558}. The electron from reduced FAD is then transferred to a proximal heme group, a distal heme and ultimately to molecular oxygen. The oxygen is the final electron acceptor and is reduced to form superoxide anion (Vignais, 2002).

The cytosolic subunits $p67^{phox}$, $p47^{phox}$, and Rac2 are required for superoxide production *in vivo* as demonstrated by naturally occurring mutations in the genetic disorder CGD, while the role of $p40^{phox}$ is less clear. It has been shown in cells that these proteins exist as a complex and translocate to the membrane to interact with cytochrome b_{558}. Each of these cytosolic components contains an SH3 domain which binds to proline-rich regions on $p22^{phox}$, $p47^{phox}$ and $p67^{phox}$, however the exact mechanisms by which

these proteins interact and activate the oxidase are unknown (Lapuge, 2000). $p47^{phox}$ is thought to serve as an adaptor protein to facilitate binding of $p67^{phox}$ and flavocytochrome b. $p67^{phox}$ is thought to be a critical activating component of the oxidase complex, binding directly to flavocytochrome b via an activation domain.

Role of Rac2 in the NADPH Oxidase Complex

The role of Rac in the NADPH oxidase is thought to be both as an activator and accessory protein that facilitates the correct orientation of the interacting proteins. Like the other cytosolic subunits $p47^{phox}$ and $p67^{phox}$, Rac translocates to the membrane after neutrophil activation (Quinn, 1993). Rac activation is tightly regulated to ensure that the NADPH oxidase does not produce toxic oxygen products unless they are needed in an immune response. There are several families of proteins that regulate the activation of Rac, including the Guanine nucleotide exchange factors (GEFs). The GEF involved in the oxidase has been reported as Vav-1 (Price, 2000). Elegant studies using isothermal titration calorimetry have shown that Rac is only able to activate NADPH oxidase when it is bound with GTP (Lapouge, 2000). Rac1 and $p67^{phox}$ been co-crystallized by Lapouge et al for structure determination of the complex and identify contact regions between the oxidase components.

There are two “switch domains” in Rac that are equivalent to regions found in the small GTP binding protein Ras (Freeman, 1994). Switch I on Rac is most likely involved in activating the NADPH oxidase. Upon binding with GTP, Switch I undergoes conformational changes resulting in interaction with the cytosolic subunit $p67^{pohx}$ (Lapouge, 2000). Rac2 and $p67^{phox}$ also interact via a tetratricopeptide repeat (TPR)

motif (Dang, 2000). TPR motifs are degenerate 34 amino acid sequences found in many proteins and are arranged in tandem arrays of 3-16 motifs. TPRs may act as scaffolds for the assembly of multi-component protein complexes and mediate protein-protein interactions in other systems such as the anaphase promoting complex (APC) (Das, 1998). The TPR is located on the N-terminus of $p67^{phox}$ and is required for interaction with Rac as determined by mutagenesis of the four regions where the characteristic motif is found.

Non-Oxidative Neutrophil Killing

Once neutrophils migrate to sites of infection, they are able to directly engage pathogens and eliminate such agents by both oxidative and non-oxidative pathways. Receptors on the surface of neutrophils are able to bind to compounds often found on the surface of invading pathogens. Fc and C3b receptors on neutrophils bind to immunoglobin and C3b molecules, respectively, which act as opsonins to coat foreign particles for recognition by immune cells. The particles are recognized and internalized into a membrane bound phagosome. A critical role for Rho-family GTPases in regulating phagocytosis has been clearly documented. Macrophages and neutrophils also have a variety of different granules which contain proteins and peptides that facilitate the antimicrobial response. During cell killing, the phagosome fuses with these granules and bacteria are then killed by chemical and enzymatic processes. The role of Rho family GTPases in mediating these fusion events will be outlined in the following section.

Of final interest, a novel non-oxidative killing method has been identified by Brinkmann et al. which the group coined “neutrophil extracellular traps” or NETS.

These extracellular structures are excreted out of the neutrophil and trap bacteria in a web of DNA and bound proteins. Bacteria trapped in NETS presumably experience a high local concentration of killing agents such as the proteolytic enzyme elastase. Histones, which have been shown to be bactericidal in both vertebrates and invertebrates (Patat, 2004), are also present in NETS. Both gram positive and gram negative bacteria were shown to be susceptible to NETS. Examination of tissue sections obtained from patients with appendicitis showed the presence of NETS, suggesting they are a physiologically relevant immune mechanism of neutrophils (Brinkmann, 2004).

Neutrophil Granule Types

Neutrophils contain four granule types: primary azurophilic, secondary specific, tertiary granules, and secretory vesicles. Each granule type responds to a specific intracellular calcium spike associated with the activation of the neutrophil and fuses with the phagosomal membrane to release the contents of the granule either to kill phagocytosed bacteria, or with the plasma membrane of the cell to release the toxic contents into an area containing bacteria outside of the cell (Abdel-Latif, 2004).

Not surprisingly, since Rac2 is an established component in neutrophil chemotaxis and other cytoskeleton remodeling events, it has been shown that Rac2 is critical for neutrophil granule exocytosis. Rac2 and Cdc42 are also involved in mast cell degranulation (Brown, 1998). It has been shown that *rac2*$^{-/-}$ neutrophils develop physiologically normal granules, but without Rac2, they cannot release their primary granules. There are many known instances of functional overlap between Rac1 and Rac2, but this study uncovers a divergence in function between Rac1 and Rac2.

Rac2 Regulates the Actin Cytoskeleton

Actin Polymerization Basics

The activation of Rac drives the polymerization of actin through interactions that have been described as a 'black box' (Schmitz, 2000). Actin exists in two oligomeric states, monomeric G-actin and polymerized filamentous actin (F-actin). The actin amino acid sequence is highly conserved between species. Actin polymerization, the polymerization of G-actin into F-actin, occurs spontaneously at the high concentrations present *in vivo*, so actin is regulated by a variety of actin binding proteins which sequester actin and inhibit self-assembly. Actin molecules are structurally polarized; they are asymmetrical protein subunits which assemble at the plus end of the filament due to binding energetics, while most depolymerization occurs at the minus end. The plus end of actin filaments are guarded by capping proteins which are released by increased concentrations of the phospholipid PIP_2. Rac activates PI 5-kinase, which may contribute to uncapping at the barbed ends of actin filaments through the generation of PIP_2, leading to membrane extension.

Among the most important actin binding proteins are the Arp 2/3 protein complex. This complex allows new actin filaments to branch off at 70^o angles from existing actin filaments and also nucleates new actin filaments that do mechanical work and actually push the leading edge of the cell forward (Janmey, 2004). Rac is an upstream activator of the Arp2/3 complex and activates Arp2/3 by the action of WAVE/SCAR. PIP_2 is also a mediator of actin polymerization through the activation of the WAVE complex, although

PIP_3 binds preferentially. Scar/WAVE proteins are not bound directly by Rac1, but assemble into multiprotein complexes with Specifically Rac1-Associated protein-1 (Sra-1) and Nap1. Active Rac1 has the ability to cause the proteins Sra-1, Nap1, WAVE2 and Abi-1 to form stable complexes *in vivo* as determined by immunoprecipitation of cells activated by AIF treatment or by expression of constitutively active Rac. Removal of Sra-1 or Nap1 by RNAi treatment in cells abolishes the ability of Rac to form lamellipodia and overexpression of WAVE2 or injection of constitutively active L61Rac1 cannot restore growth factor induced membrane protrusions (Steffen, 2004).

Multiple Signaling Pathways Exist

One mechanism proposed by Janmey and Lindberg for the involvement of phosphoinositides in the regulation of actin polymerization suggests that Rac or possibly another small GTP binding protein first activates PtdInsP kinase, which moves to the membrane via a dibasic motif at its tail and generates a locally increased concentration of PIP_2. N-WASP is then recruited to the area of high PIP_2 concentration and binds the lipid (Tolias, 2000). This binding, either alone or possibly with Cdc42, leads to conformational changes in WASP that release auto-inhibitory interactions, allowing the Arp2/3 complex to bind WASP and nucleate new actin filaments, leading to membrane protrusion (Janmey, 2004). PIP_2 also induces inhibitory conformational changes in the structure of gelsolin, a protein responsible for severing and capping actin filaments. The ability of PIP_2 and PIP_3 to initiate actin polymerization explains why actin polymerization events can occur despite treatment with PI3K inhibitors such as wortmannin, depending on the membrane receptor responsible for upstream signaling.

Rac Causes Actin Polymerization

It is thought that activation through Rac biases the localized actin polymerization around the areas of lamellipodium formation. Localized activation of Rac is probably due to the activation of Rac guanine nucleotide exchange factors by locally produced PtdIns (3,4,5)P_3 or direct receptor activation (Welch, 2003). Positive feedback loops may amplify the local signal once Rac is activated, as Rac has been suggested to stimulate or recruit PI3K at the membrane, leading to the production of PtdIns(3,4,5)$P_{3,}$ which regulates at least two mammalian Rac GEFs, PREX1 and PIX (PAK-interactin exchange factor) (Welch, 2002). Interestingly, it has been shown that in any given population of these lipid molecules that influence actin polymerization, there are distinct lipid pools, and only a small population of the cellular phosphoinositide could be hydrolysed, phosphorylated, or dephosphorylated in response to a stimulus (Janmey, 2004),

Hypothesis and Objectives

Rac2 May Interact Directly with Actin

Rac is a central component in neutrophil function. Rac regulates many cellular functions including motility, activation, NADPH oxidase, and cytoskeletal rearrangements. Previous studies from this laboratory have suggested that Rac can bind directly to actin. The purpose of this study was to identify the binding site for Rac2 and actin and determine if Rac binding caused actin polymerization. It has been convincingly shown that a similar small GTP binding protein, Rap2, binds directly to the actin cytoskeleton (Torti, 1999). In these studies, Rap2 was incorporated into the cytoskeleton

during actin polymerization assays and cytoskeletal actin was shown to bind to a column of immobilized Rap2. Rap2 and Rac2 are 34% identical and share many important binding domains. Our data (this study and previous observations, published and unpublished) suggest that Rac2 also interacts with the actin cytoskeleton in a direct manner. The major protein motif we suggest is responsible for interactions with actin, KXDXR, is KXDXE in both Rap2 and Rac2 R120E. The Rac2 R120E mutant was shown to bind actin with a higher affinity than wild-type Rac2 (Jesaitis et al., unpublished data). A sequence alignment of this region shows that Rac2 R120E has high local identity to Rap2, a known actin binding Ras GTPase (Figure 2).

```
RAP2A       110-   PVILVGNKVDLESER
RAP2B       110-   PMILVGNKVDLEGER
RAB3B       129-   QVILVGNKCDMEEER
RAB14       118-   VIILIGNKADLEAQR
Rac2Emut    109-   PIILVGTKLDLEDDK
                    :**:*.* *:* ::
```

Figure 2. Sequence alignment showing the KXDXE motif in small GTPases from the Ras super family. The sequence identity is quite high between Rac2 R120E and Rap2, which has been shown to bind actin directly. `*` represents identical amino acids; `:` highly similar amino acid substitution; `.` moderate similarity in amino acid substitution. Sequence alignment generated by ClustalW.

Thus, we hypothesize that small GTPases of the Rho family bind directly to G- or F-actin to modulate its cellular function. To this point, unpublished data from the Jesaitis group and the above study with Rap2 represent the only known information describing direct actin binding as a novel regulatory function of small G-proteins. In the present

study, phage display technology was used to attempt identification of amino acid residues on the surface of actin that might directly mediate interactions with Rac2. In addition, a mammalian cell expression system was developed for future studies exploring the possible functional effect of Rac2 and Rac2 mutants on actin polymerization in intact cells.

CHAPTER 2

MATERIALS AND METHODS

Purification of GST-Rac2 and GST-Rac2 R120E from *E. coli*

Rac Purification

The *E. coli* expression vector pGEX-2T containing the human Rac2 gene cloned downstream of the GST tag was obtained from Dr. Mark Quinn. This construct contains a Cys-Ser mutation at Rac2 Cys 189. The Rac2 R120E mutation was generated by K. Stone at Montana State University. The *E. coli* strain BL21-DE3 was used for overexpression from the plasmid pGEX-2T for both wild-type Rac2 and Rac2 R120E. The expression plasmid was under positive selection by virtue of an ampicillin resistance gene. For protein expression, cultures were started from glycerol stocks (stored at –70^{o}C) in 4 mL tubes of LB containing 50 μg/ml ampicillin overnight with shaking at 37^{o}C. Overnight cultures were then added to 1 L LB also containing ampicillin. Cells were grown at 37^{o}C to an OD_{600}~0.7 and then were incubated for an additional 3 hours at 22^{o}C following induction with 100 μM IPTG. For overexpression of GST-Rac2 R120E, cells were induced for ~16 hours at 18^{o}C with 100 μM IPTG. This procedure substantially improved the yields of soluble protein. Following induction, cells were harvested by centrifugation and stored at -20^{o}C until further use.

For purification, frozen cell pellets from 1L of culture were homogenized in 20 ml of 20 mM Tris (pH 7.4), 100 mM NaCl, 4 mM $MgCl_2$, 1 μM GDP, 1% TX-100, 1 mM PMSF, 1 mM DTT and 20 μl Sigma Mammalian Protease Inhibitor Cocktail

(Resuspension buffer). DNAse and lysozyme were then added (100 μg/μl final concentration) and cells were further homogenized. Resuspended cells were then sonicated on ice 5 x 5 seconds using a Fisher Scientific sonic dismembrator model number XL2005 at the setting of 3. Following removal of insoluble material by centrifugation at 113,600 x g in a Ti60 rotor for 30 min. at 4^{o}C, soluble material was applied to glutathione-agarose beads overnight at 4^{o}C with tumbling. Preparation of glutathione-agarose beads was performed just prior to application of soluble material. For equilibration, beads were rinsed with dH_20 and then blocked with 1% gelatin to prevent non-specific protein binding. The blocked beads were then washed with 20 ml of PBS followed by 20 ml of 20 mM Tris, 100 mM NaCl, 4 mM MgCl2, (pH 7.4). Beads were then equilibrated with Resuspension buffer prior to addition of soluble extracts.

Following the overnight incubation of *E. coli* soluble extracts and glutathione-agarose beads, unbound material was removed and the beads were then washed with 15 ml of Resuspension buffer. Beads were then washed two additional times with 15 ml of 20 mM Tris, 100 mM NaCl, 4 mM $MgCl_2$, 1 μM GDP, and 1% octyl glucoside. All washes were performed at 4^{o}C. GST-Rac2 was eluted with 2 ml of 50 mM Tris, 100 mM NaCl, 4 mM $MgCl_2$, 1 μM GDP, 1% octyl glucoside, 20 mM reduced glutathione, (pH 8.5) (Elution buffer). It is important to note that the addition of glutathione causes a large drop in the pH of the buffer, so pH must be adjusted after glutathione is added. Following purification of GST-Rac2, the protein was dialyzed against 2 L of 25 mM Tris, 100 mM NaCl, 5 mM $MgCl_2$, 1 mM EDTA, and mM DTT, (pH 7.4) (Dialysis buffer) overnight at 4^{o}C. SDS-PAGE analysis was used to evaluate the purity, and molecular weight of the

Rac2 following isolation. After dialysis to remove glutathione (which causes a high background reading), the samples were analyzed for protein content using absorbance spectroscopy. The extinction coefficient (280 nm) of the GST-Rac2 fusion protein was estimated to be 50,690 $M^{-1}cm^{-1}$ by the program ProtParam and was used for accurate determination of the protein concentration at 280 nm. Purified protein was stored at -20^{o}C until it was needed.

Large Scale GST-Rac2 Purification

The amount of purified Rac needed for subsequent applications exceeded the capacity of the GST-Rac2 purification outlined above, so the protocol was scaled up with a few modifications to increase overall yield and efficiency from this procedure. Identical bacterial strains, and materials were used in the large scale purification.

Overnight cultures of GST-Rac2 expressing *E. coli* were grown at 37^{o}C with vigorous shaking in 400 ml LB with ampicillin. This broth was used to inoculate four one liter flasks of LB with ampicillin. The cultures were grown in baffled flasks at 37^{o}C until OD_{600} of 0.6, at which time they were induced with 100 μM IPTG for 3 hours at 22^{o}C for GST-Rac2 or for ~16 hours at 18^{0}c FOR gst-Rac2 R120E. After cells were harvested by centrifugation, pellets were homogenized in 80 ml Resuspension buffer containing DNAse and lysozyme and frozen at -20^{o} overnight. The next morning, the thawed cell lysate was sonicated 5 x 5 seconds on ice in 10 ml aliquots. The cell lysate was then cleared by centrifugation 113,600 x g for 30 minutes at 4^{o}C. The clarified cell lysates were added to 1.5 ml of Glutathione agarose beads (which had been previously prepared as described above) and the mixture was tumbled gently for 2 hours at 4^{o}C. Beads were

then collected in a small plastic column and the cell lysate supernatant was removed. Beads were then washed with 4 x 40 ml of Resuspension buffer with 1% octyl glucoside instead of the detergent TX-100. Following this procedure, the last fraction of bead wash buffer was checked by absorption spectrometry to ensure that residual absorption due to TX-100 and nucleic acids had reached baseline levels.

For protein elution, the glutathione beads are tumbled gently for 15' at 4^{o}C following addition of 4 mL of Elution Buffer (pH 8.5). A second elution step was also performed to remove additional protein from the matrix. Elution fractions were pooled and dialyzed overnight in 10,000 MW cutoff cassettes (Pierce Slidalyzer) against 2L Dialysis buffer. Dialysis buffer was changed 3 times to remove detergent and glutathione. Purified GST-Rac2 and Rac2 R120E was analyzed using absorption spectroscopy and SDS-PAGE and was stored in aliquots at -20^{o}C until needed as previously described.

GTPγS Binding Analysis

In order for Rac2 to initiate cellular response, it must be bound to GTP, which changes the conformation of Rac. To determine if the Rac over expressed in *E. coli* binds ligand in a concentration dependent manner, GTPγ[^{35}S] binding assays were performed on both Rac2 and Rac2R120E. By examining the GTP binding activity and kinetics of Rac2, we can determine the structural integrity of overexpressed protein.

GTPγ[^{35}S] was purchased from Amersham through the Radiation Safety Department of MSU. Stock solution was stored in small aliquots at –80^{o}C. Unlabeled GTPγS (Sigma) was made in Buffer A (25 mM Tris, 100 mM NaCl, 4 mM $MgCl_2$ pH 7.4), stored in small aliquots and used fresh. For preparation of the nucleotide mix, 1 μl of

GTPγ[^{35}S] (approximately 2.4 x 10^6 counts per minute) was added to 70 μl of 0.5 mM cold GTPγS. This was enough nucleotide mix was enough for a 3.2 ml total reaction volume used to collect the multiple time points in these assays. For GTPγ[^{35}S] binding assays, 100 pmol of GST-Rac2 was diluted into Buffer A. The mixture was then brought to 7.5 mM EDTA and incubated for 5 minutes at 30^{o}C in order to release any bound nucleotide remaining after purification. The nucleotide mix was then added to the reaction and samples were incubated for various time points before the reactions were quenched with 20 mM $MgCl_2$ which inhibits dissociation of bound nucleotide. After the above incubations, the protein- nucleotide mixture was filtered through a glass-filter membrane (Whatman) to retain the protein along with any GTPγ[^{35}S] bound to Rac2. Filter membranes were either washed twice with 1.75 ml Buffer B, to ensure any GTPγS remaining in the sample was bound to Rac2 or the membranes were not washed to examine the possibility that the GTPγS could dissociate from Rac2 easily due to *in vitro* conditions. Glass filters were placed in 10 ml glass scintillation vessels and immersed in 5 ml Scinti-Safe 30% (Fisher). GTPγ[^{35}S] was quantified in a Beckman Scintillation counter

Fluorescence spectroscopy for analysis of Rac conformation

Fluorescence measurements were conducted in UV-transparent microcuvettes at room temperature with the excitation monochromator set at 280 nm and the emission spectrum scanned between 300-400 nm. The slit width for both monochromators was set at 2 nm, corresponding to 4 and 8 nm bandpass for the excitation and emission monochromators, respectively. The fluorescence emission spectrum of Rac2 and Rac2R120E was

measured to determine if the structural conformation of the wild type and mutant protein were similar. Because the mutant protein Rac2 R120E does not bind ^{35}[S] GTPγS, it was difficult to determine if the mutant protein had a low affinity for GTP or if the overall structure of the mutant was mis-folded. Shifts in protein conformation associated with the addition of denaturing agents are measured by comparison of fluorescence emission spectrum taken under different conditions.

Phage Display Analysis

Phage Display Column Protocol

Phage display was performed using 1.5 mg of purified Rac2 that had been extensively dialyzed into PBS. For preparation of the affinity matrix, Rac2 was diluted into 2.2 mL 0.1 M $NaHCO_3$, 0.5 M NaCl (pH 8.3) (Coupling buffer) and then applied to 0.3 g of CNBr-activated Sepharose beads (which had been prepared according to manufacturer's directions), overnight at 4^{o}C. After the reaction and removal of the reaction buffer, the beads were washed with 25 ml Coupling buffer. Beads were then washed with 10 ml of 1 mg/ml BSA, 0.5% Tween 50 mM Tris-Cl, 150 mM NaCl (pH 7.5) (Phage Buffer). After washing, the beads were resuspended in 500 μl of Phage buffer. One third of the GST-Rac2-coupled beads were transferred to a tube containing 1 ml of Phage buffer. The remaining two thirds of the beads were stored in 0.02% azide at 4^{o}C for later use. About 10^{12} plaque forming units of the phage library JB 404 (graciously provided by Dr. Jim Burritt) was added to the first third of the beads and tumbled at 4^{o}C overnight. The beads were washed the next morning with 100 ml of cold Phage buffer. After extensive

washing, phage adherent to the Rac2-Sepharose beads were eluted from the column by adding 1 ml of 1 mM GDP in Phage buffer (GDP Elution Buffer). The elution was neutralized by adding 70 ul of 2 M Tris base. This elution is referred to as the first round elution. 50 ul of the first round eluate was saved for titering.

The remaining first round eluate was added to 15 ml of early stationary phase *E. coli* K91 cells and allowed to infect for 15 minutes at room temperature. After this, the phage/*E. coli* mixture was mixed with 45 ml of melted soft agar and poured over a 9x13 inch sheet of LB agar in a baking dish. The large dish was incubated at 37^{o}C overnight. In the morning, the agar was almost confluent with phage plaques.

To collect the phage, the baking dish was covered with 40 ml of 50 mM Trisl, 150 mM NaCl pH 7.5 (TBS) and rocked at room temperature for 2 hours. The TBS was collected and spun at 12,000 x g for 20' at 4^{o}C two times to remove any residual cells. The resulting supernatant was transferred to a new tube and 0.15 volumes of PEG-NaCl were added and the solution was set on ice for 4 hours. The solution was then spun as above and precipitated phage were collected and resuspended in 1 ml TBS. The phage were transferred to a microfuge tube and 150 ul of PEG-NaCl was added. The solution was set on ice for one hour, microfuged for 2 minutes and resuspended in 300 ul of TBS. This sample was referred to as first round amplified phage.

For further selection, one half of the reserved beads from above were washed and 100 ul of the first round amplified phage were added to 1 ml of Phage buffer and applied to the Rac2-Sepharose beads. The basic protocol from above was repeated for the second and third rounds of phage selection.

After the second amplification, the third round eluate was brought to 0.01% azide and stored at 4^{o} C. Titers were performed on all three rounds of phage eluate to determine if positive selection was occurring. The third round eluate was plated at 10^{-7} and 10^{-8} dilution in soft agar to isolate individual colonies for phage purification and sequencing.

Because no strong consensus sequence was obtained by eluting phage from GST-Rac2 or GST-Rac2 R120E with 1 mM GDP, two subsequent phage display experiments were performed on GST-Rac2 R120E using alternate Phage elution buffers. The first method used 500 μl of High Salt Buffer (2M NaCl, 2 mM EGTA) to elute phage from each of the three selection rounds. After the high salt elution buffer was collected, it was immediately diluted twenty-fold with sterile water to reduce the NaCl concentration to 100 mM. The protocol for high salt elution was carried out for three rounds of amplification and selection as described for the GDP phage elutions. The second method used the same CnBr-Sepharose GST-Rac2 R120E beads that had been previously eluted with high salt. The beads were washed with 10 mL phage buffer and eluted with 2 mL 0.1 M glycine pH 2.2 (Low pH Phage Elution buffer). The phage display analysis protocol was followed as above for the High Salt Buffer, with the Low pH buffer elution being carried out on the same GST-Rac2 R120E beads after each High Salt elution.

Purification of individual phage and DNA isolation

The third round eluate from the phage display experiment was screened to isolate phage clones in order to sequence the DNA coding for the nine amino acid variable tail of the phage that bound with high affinity to Rac2 and Rac2R120E affinity columns. For

isolation, the eluate was serially diluted and plated on soft agar to isolate individual plaques growing on a lawn of K91 *E. coli* cells. Isolated plaques were inoculated into 2 ml of LB broth with 75 μg/ml kanamycin and incubated with shaking overnight at 37^{o}C. Following growth, cultures were centrifuged to remove bacterial cells and the resulting supernatants were transferred to new microcentrifuge tubes.

Both a QIAprep Spin M13 kit and a precipitation method were used to purify single-stranded M13 DNA. The QIAprep protocol was provided by the manufacturer. Briefly, a 1/100 volume of MP is added for M13 phage precipitation and this mixture is incubated for 2 minutes at room temperature. The mixture is then applied to a QIAprep spin column and microfuged to retain the phage on the silica-gel membrane. Buffer MLB is applied to the membrane twice to lyse the bound phage. The column is then washed once with buffer PE to remove residual salt from the membrane. After 10 minutes of incubation, M13 phage DNA was eluted from the column in 100 μl of 10 mM Tris, (pH 8.5). As an alternative approach, a precipitation method was also used to purify phage. In this procedure, 1.25 ml of culture supernatant was mixed with 138 μl 40% PEG-8000 and 138 ul 5 M NaOAC (pH 7.0) and then incubated for 2 hours on ice. This precipitation mixture was then spun at 14,000 rpm in a microcentrifuge for 15 minutes and aspirated to remove supernatant from phage pellet. The pellet was spun a second time to ensure all supernatant was removed. The pellet was then resuspended in 30 μl 10 mM TE (pH 5.0) and incubated in a boiling water bath for two minutes to disrupt protein contaminants prior to sequencing.

Sequencing Reactions

Purified M13 phage clones were sequenced with a Thermo Sequenase Radiolabeled Terminator Cycle Sequencing Kit (USB) using two different protocols, one employing a thermocycler and a second technique that relies on a single reaction cycle. The protocol using a thermocycler provided much better signal intensity and reproducibility in the author's hands. The sequencing reactions used the primer 5'-gttttgtcgtctttccagacg-3' to obtain chain elongation of the variable nonapeptide-coding region of the M13 phage. Cycling termination reactions were prepared according to the guidelines suggested by USB. Briefly, 2 ul Reaction buffer, approximately 250 ng of ssDNA, 1 pmol of the above primer, 8 units Thermo Sequenase polymerase and Millipure H_2O to 20 μl were divided into four aliquots. Each tube was then mixed with 2 μl of Nucleotide Master Mix and 0.5 μl of an individual dideoxy-nucleotide (ddNTP) base labeled with [α-^{33}P] immediately before being layered with mineral oil heat cycled in a MiniCycler (MJ Research, USA) thermocycler. The temperature cycle parameters were 30 seconds at 95^{o}C, 30 seconds at 55^{o}C, 90 seconds at 72^{o}C, repeat 20 times and then hold at 4^{o}C. After thermal cycling was complete, 4 μl of stop solution was added to each tube.

For the single heat cycle sequencing technique, 2 μl reaction buffer, 250 ng ssDNA, 0.5 pmol primer, and 2 units Thermo Sequenase polymerase were heated to 65^{o}C for 2 minutes and allowed to cool slowly. Following a brief spin, of 2.5 μl of Nucleotide Master Mix, and 0.1 μl [α-^{33}P] ddNTP were added to the cooled DNA mixture. This mixture was then heated to 72^{o}C to allow termination chain labeling and the reaction was stopped with 4 μl stop solution.

Sequence Analysis by Denaturing Gel Electrophoresis

DNA sequencing gels require a delicate touch and precise sample handling. The gel apparatus used in these experiments was a Gibco BRL Sequencing Systems Model S2 gel box and a BioRad Powerpac 3000 power supply. An 8% acrylamide solution (20:1 acrylamide, bis-acrylamide) containing 7.5 M urea (to denature the DNA) in Glycerol Tolerant buffer (89 mM Tris, 28 mM taurine, 0.5 mM EDTA) was mixed and polymerized between glass electrophoresis plates with 0.1% ammonium persulfate and 0.025% TEMED. The acrylamide gel was loaded into the electrophoresis apparatus, then Glycerol Tolerant buffer was added and the gel was pre-heated to 55^{o}C. DNA sequencing reactions were loaded and the gel was resolved at 60-65 mA. Gel temperature was kept between 50-55^{o}C during electrophoresis by adjusting power if needed. The sequencing gel was stopped after the dye front had progressed two-thirds of the way down the sequencing gel, and the gel was fixed in 5% acetic acid, 20% methanol for 1 hour followed by drying in a BioRad Model 583 Dryer. Once the acrylamide gel was dry, it was placed in a Molecular Dynamics Storage Phosphor Screen for one to three days. After exposure, the cassette was read in a Molecular Dynamics phosphor imaging device. Sequences were manually read from phosphor images and recorded for analysis

Computational Methods

Data generated from phage display analysis was modeled to human actin using the computer programs FINDMAP and Deep View- Swiss PDB Viewer. FINDMAP and EPIMAP, an updated version, are a computer programs designed to predict three dimensional binding epitopes by comparing the amino acid probe sequences (selected

phage) against the amino acid sequence of a target protein. This program is designed to predict discontinuous epitope regions that form a protein-protein interaction site by permitting large gaps in the target sequence (actin in the present study) during alignment. FINDMAP was developed at Montana State University and was first reported by Mumey et al, 2003 and Bailey et al., 2003.

In order to obtain a three-dimensional model of human actin, the amino acid sequence of human actin, the amino acid sequence of human actin was modeled on the known structure of rabbit actin. The program Swiss PDB viewer is a publicly available protein modeling program for protein structure. The user can begin with a known protein structure and make mutations in selected amino acid residues. Swiss PDBViewer is available over the world wide web at: http://www.expasy.org/spdbv/.

Rac2 Expression in Mammalian Cells

Cloning Methods

Cloning of Rac2 and Rac2 R120E into the pGene vector for mammalian expression was conducted as follows. The Rac2 and Rac2R120E genes were isolated from pGEX-Rac2 and pGEX-Rac2 R120E vectors) by digestion with BamHI and EcoRI. The resulting fragment was isolated by agarose gel electrophoresis and gel purification using the Qiagen gel purification kit (Qiagen, Valencia, CA). The Rac2 and Rac2 R120E genes were ligated into the pGene vector (Invitrogen, Carlsbad, CA) using the BamHI and EcoRI sites and ligation reactions were electroporated into *E. coli* XL1-Blue. Following transformation, cells were plated on LB agar/ 100 μg/mL ampicillin and single colonies

were grown in LB/ampicillin overnight at 30^{o}C. After cell growth, frozen stocks were prepared and cells were screened for insert b restriction digestion (EcoRI/BamHI) of purified plasmid DNA. Constructs containing the insert were sent to Davis Sequencing for DNA sequence analysis (forward and reverse strands were sequenced). DNA Sequence analysis revealed a cysteine to serine mutation used to prevent cysteine to cysteine disulfide bonds during expression of GST-Rac2 and GST-Rac2 R120E in *E. coli*. This mutation would prevent normal protein function in mammalian cells, as this region is critical for membrane localization. Using the newly generated pGene vectors containing Rac2 or Rac2 R120E as the source of DNA, the Quickchange Mutagenesis kit (Stratagene, La Jolla, CA) was used according to manufacturers instructions to induce mutation of the serine back to a cysteine (5' mutagenic primer: 5' CGGCAGCAGAAGCGCGCCTGCAGCCTCCTCTAGGAATTC 3'; 3' mutagenic primer: 5' GAATTCCTAGAGGAGGCTGCAGGCGCGCTTCTGCTGCCG 3'). PCR conditions were as follows: step 1: 95^{o}C for 1 minute, step 2: 95^{o}Cfor 30 seconds, step 3: 72^{o}C for 7 minutes, 30 seconds, step 4: 17 times to steps 2, step 5: hold at 4^{o}C. Following PCR mutagenesis, the resulting products were electroporated into E. coli XL1-Blue and resulting transformants were grown for purification of plasmid DNA using a QIAprep Spin Miniprep kit (Qiagen, Valencia, CA). PCR products were analyzed by DNA sequence analysis (Davis Sequencing) to ensure fidelity of the gene.

Because Rac1 is expressed in all cells and the high identity between Rac1 and Rac2 causes frequent antibody cross-reactivity, a C-terminal c-myc tag was inserted to facilitate identification of overexpressed Rac2. The GST-Rac2 and GST-Rac2 R120E

vectors with the cysteine described above were used for linker PCR mutagenesis using the 5' primer (5' CCCCTGCTATTCTGCTCAACCTTCC 3') and the 3' primer (5' CGATAGCGGCCGCCTACAGGTCTTCCTCGGAGATCAGCTTCTGCTCGAGGAG GCTGCAGGCGCGCTTCTGC 3'). Thermocycler reaction conditions were as follows: step 1: 95^{o}C for 1 minute; step 2: 95^{o}C for 30 seconds; step 3: 65^{o}C for 1 minute; step 4: 72^{o}C for 2 minutes; step 5: go to step 2 17 times; step 6: 95^{o}C for 30 seconds; step 7: 65^{o}C for 1 minute; step 8: 72^{o}C for 5 minutes; step 9: hold at 4^{o}C. Following PCR linker mutagenesis, the resulting products was digested with Kpn1 and NotI, gel purified using the QIAgen gel purification kit and ligated into the pGene vector which had also been double digested and gel purified. The c-myc tag was also added to the N-terminus of Rac2 and Rac2 R120E with linker PCR mutagenesis using the 3' primer (5' CGATAGCGGCCGCCTAGAGGAGGCTGCAGGCC 3') and the 5' primer (5' CTATGGTACCCACTATGGAGCAGAAGCTGATCAGCGAGGAGGACCTGCAGGC CATCAAGTGTGTGGTGGTGG 3'). Thermocycler reaction conditions were identical to those used for the C-terminal c-myc tag. Products of the PCR reactions were purified using agarose gel purification (Qiagen, Valencia, CA) and were ligated into the pGene vector. DNA sequence analysis was performed in the forward and reverse directions to confirm the sequence of all generated constructs.

Cell Culture and Transfections

HEK291 cells were cultured in Dulbecco's modified Eagle's medium containing 10% FBS (Invitrogen), 50 units/ml penicillin, 50 µg/ml streptomycin and 50 µg/ml hygromycin. HEK291 cells were transfected using LipofectAMINE 2000 (Invitrogen)

with pGene plasmids containing DNA for c-myc Rac2 or c-myc Rac2R120E (myc tag at the N-terminus) using Opti-MEM medium (Invitrogen) as per Invitrogen protocol recommendations. HEK cells were cultured without antibiotics for 24 hours prior to transfection in six well plates containing poly-l-lysine treated coverslips. To generate regulated expression of c-myc Rac2 or c-myc Rac2 R120E (myc tag at the N-terminus), the GeneSwitch inducible expression system from Invitrogen was used. Cells were purchased with pSwitch plasmid stably expressed. Cells were transfected with 1.6 μg DNA for 24 hours. Following transfection, media was replaced and expression of pGene c-myc double transfectants was achieved by induction with 10 ng/ml mifepristone for 24 hours. The same method was employed for analysis of identical cells transformed with the pGene vector above (not containing the c-myc Rac2 insert) as a negative control

Cell Staining and Immunofluoresence

Standard inmmunofluorescence procedures were used to stain HEK cells for Rac2. Following induction, coverslips were washed with PBS to remove medium and the adherent cells were fixed for 4 minutes in freshly prepared, cold 4% paraformaldehyde in PBS. Paraformaldehyde was then removed and cold 0.4% triton X-100 (Sigma) in PBS was used to permeabilize cells for 4 minutes. Next, 1% bovine serum albumin (Sigma) in PBS was added for 30 minutes to block non-specific binding sites. Cells were then washed twice with PBS for 5 minutes. For detection of the expressed Rac protein, the anti c-myc mAb 9E10 was added to a concentration of 2 μg/ml for 45 minutes at 22^{o}C. Following this, cells were washed twice with PBS; and secondary anti-mouse mAb labeled with Alexaflour 488 (Molecular Probes, Eugene, OR) was diluted 1:500 in PBS

and incubated at 22^{o}C for 45 minutes in the dark. Coverslips were then washed twice with PBS for 5 minutes and were rinsed with water to remove residual salt before mounting on glass slides using the ProLong Antifade Kit (Molecular Probes, Eugene, OR). Slides were allowed to dry overnight at 4^{o} prior to microscopic analysis.

CHAPTER 3

RESULTS

Overexpression and Purification Introduction

In the present work, significant quantities of purified Rac2 were needed to perform experiments to demonstrate its interaction with the actin cytoskeleton. Since previous purification methods used by our group were compromised by inconsistent yields mainly due to the production of insoluble protein, modified methods had to be devised. Recombinant expression in *E. coli* was used in these studies because it is difficult to obtain large amounts of purified Rac2 from natural sources such as human neutrophils. For recombinant expression, the human Rac2 gene had been cloned into an *E. coli* expression vector with a GST fusion tag (obtained from Dr. M. Quinn) to allow for purification by affinity chromatography. Prokaryotic expression systems are convenient because they generate large amounts of protein in a short amount of time. In addition, the reagents needed to grow and purify protein with *E. coli* are inexpensive. However, *E. coli* cells are not able to add the lipid isoprenyl group found on the C-terminus of Rac2 in mammalian cells, so protein expressed in this system is not biologically identical to protein expressed in eukaryotic organisms, including humans. The overall scheme for purifying and analyzing GST-Rac2 and GST-Rac2R120E is shown as a flowchart diagram in Figure 3 and will be discussed in the following sections.

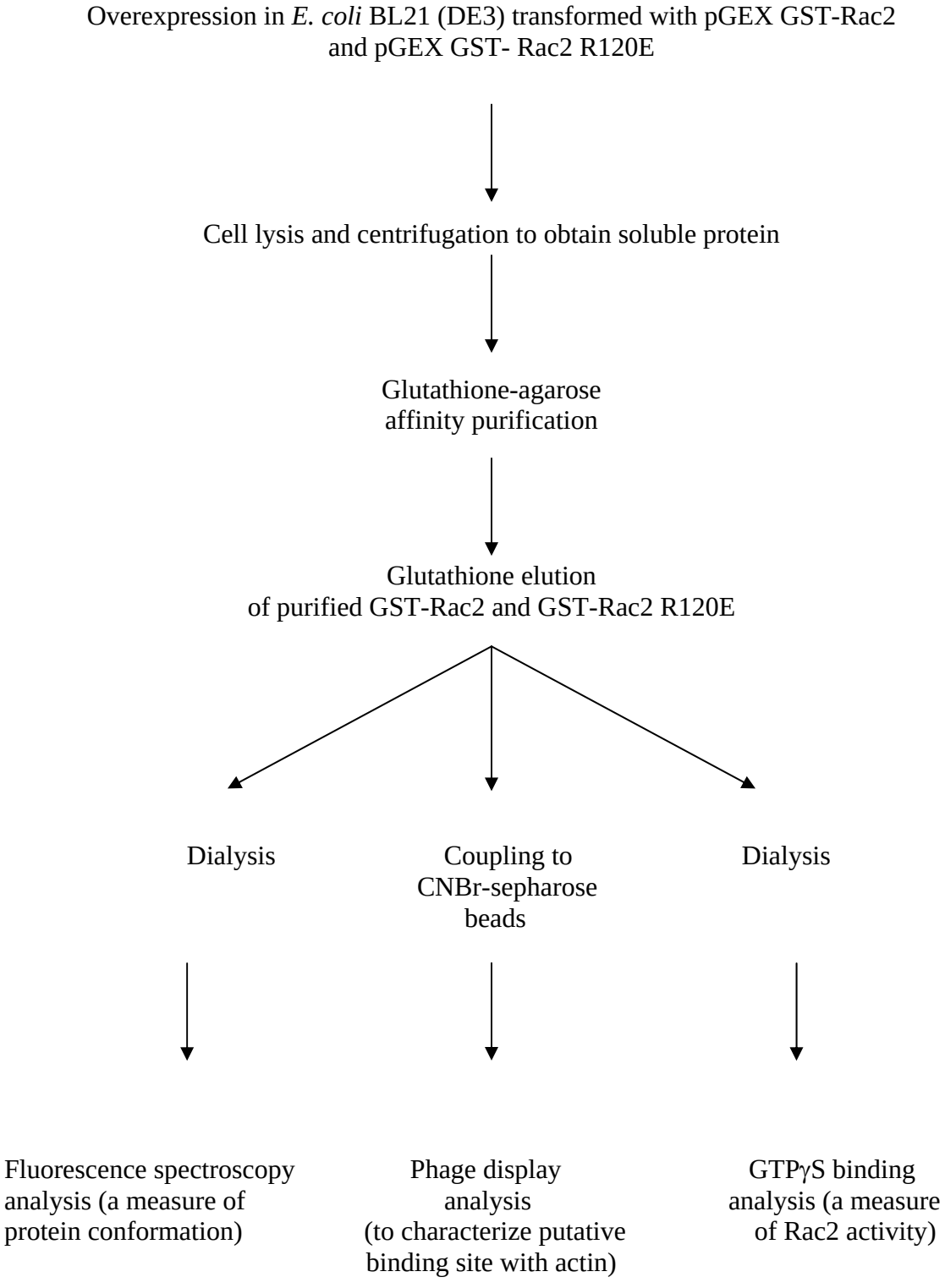

Figure 3. Strategies employed in the purification and analysis of GST-Rac2 and GST-Rac2 R120E.

Expression of Soluble GST-Rac2 and GST-Rac2 R120E

The pGEX vector used for expression of GST-Rac2 and GST-Rac2 R120E was transformed into the *E. coli* strain BL21 (DE3). Following transformation, the BL21 (DE3) cells are induced with IPTG to generate recombinant protein through the action of the T7 promoter. When IPTG is added to the medium, T7 polymerase is produced by the cells, which in turn recognizes the T7 promoter (upstream of the GST-Rac2 gene) to drive protein expression. In this system, the amount of IPTG added to the medium and the induction temperature determines the rate at which the T7 promoter is stimulated. In order to generate maximum soluble protein yields, induction studies were initially conducted with varying concentrations of IPTG added for different lengths of time. Both GST-Rac2 and GST-Rac2 R120E were produced in large quantities when cells were induced with 1 mM IPTG for 3 hours at 37^{o}C, but after cell lysis and centrifugation, most of the GST-Rac2 proteins were contained in an insoluble fraction of the cell lysate. Through optimization experiments, it was determined that maximal soluble GST-Rac2 expression occurred with 100 μM IPTG added for 3 hours at 22^{o}C. GST-Rac2 R120E was more difficult to produce, and even with the lower temperature induction (22^{o}C), most of the GST-Rac2 R120E was insoluble when cells were grown and induced as described above for the GST-Rac2. The production of predominantly insoluble protein suggests that the Rac R120E mutant may be relatively unstable and folds improperly under these induction conditions, leading to aggregates of the product with other proteins, or itself. Subsequent experiments showed that soluble GST-Rac2 R120E production

occurred best, producing milligram levels of soluble product per liter of cells, when cells were induced with 100 μM IPTG overnight at 18^{o}C.

Purification of GST-Rac2

For isolation of GST-Rac2 fusion proteins following induction, cells were lysed, clarified by centrifugation, and the soluble supernatant was bound to glutathione-agarose beads for affinity purification. After binding, the column was washed extensively to remove nucleic acids and TX-100 detergent, both of which interfere with protein concentration determination by absorbance spectroscopy. Following the column wash step, purified GST-Rac2 and GST-Rac2 R120E was eluted from the column with reduced glutathione.

Because the addition of glutathione causes a significant drop in pH of the Elution buffer, great care had to be taken to bring the pH of the elution buffer back to pH 8.5 for successful protein purification. Once induction and elution conditions were optimized, milligram per liter levels of both GST-Rac2 and GST-Rac2 R120E were produced at a high level of purity. SDS-PAGE gels showing fractions along the purification process for GST-Rac2 is shown in Figure 4. Similar results are observed during the isolation of GST-Rac2 R120E (see Figure 7).

After purification, GST-Rac2 and GST-Rac2 R120E were dialyzed extensively to remove glutathione to obtain accurate absorbance spectra in order to quantitate protein, as shown in Figure 5. Protein concentration was determined using an extinction coefficient of 50,690 $M^{-1}cm^{-1}$ (at 280 nm) obtained by analyzing the GST-Rac2 amino acid sequence

using the program ProtParam (http://au.expasy.org/tools/protparam.html). The molecular weight of GST-Rac2 (393 amino acids) is 44, 279.1 Da, according to ProtParam.

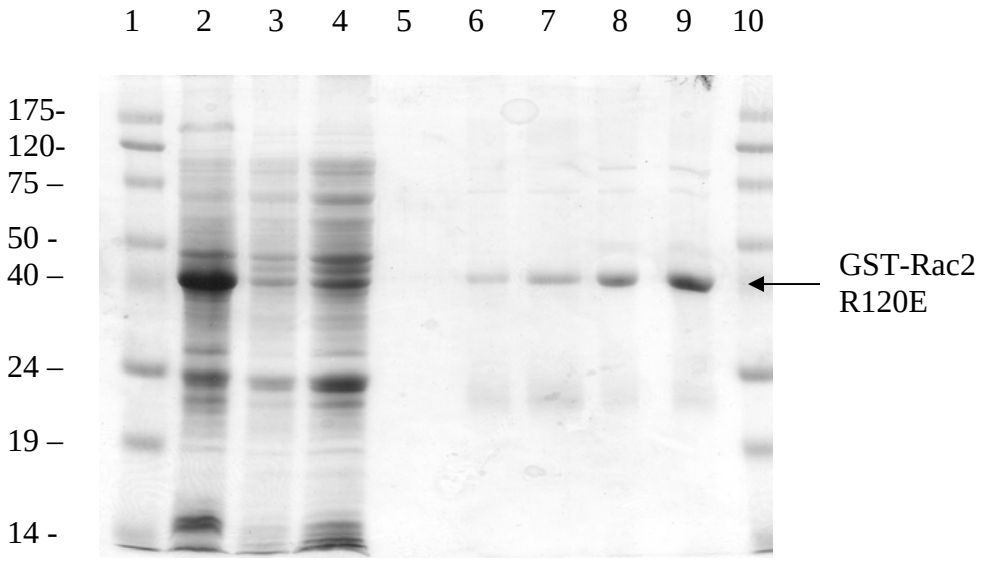

Figure 4. SDS-PAGE gel of GST-Rac2 purification from *E. coli*. Protein was detected by Comassie-Brilliant Blue staining after separation on a 12% SDS-polyacrylamide gel. Lanes 1 and 10 contain a relative molecular weight standards (in thousands); lane 2, whole cells; lanes 3 and 4, glutathione bead flow through; lane 5, wash; lanes 6-9 increasing amount of GST-Rac2 eluted with glutathione elution buffer that had been adjusted to the correct pH after the addition of glutathione.

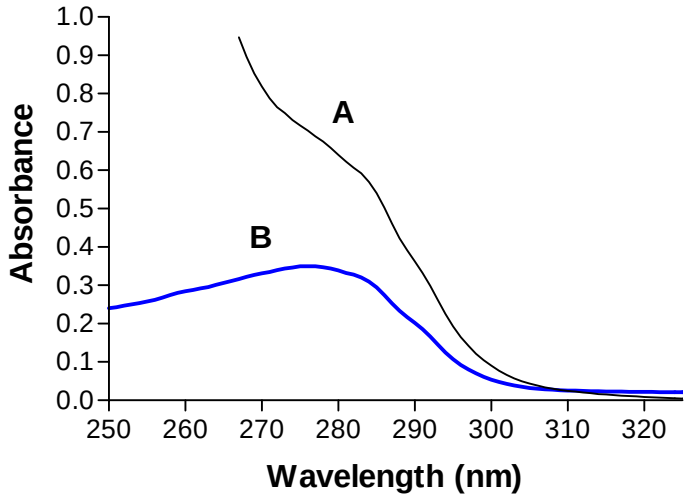

Figure 5. Absorbance spectra of GST-Rac2. Following glutathione matrix affinity purification samples of purified GST-Rac2 were analyzed by absorbance spectroscopy in Elution buffer (containing glutathione; Curve A) and following dialysis to remove glutathione (Curve B). The measurements shown in curve B were used to assess protein concentration following purification.

In attempts to isolate Rac2 in the absence of the GST fusion tag, elution from the glutathione-agarose column was also attempted through cleavage with the blood coagulation protease, thrombin. Thrombin cleaves at a site between the GST affinity tag and Rac2. Elution by thrombin cleavage was inconsistent, as the purified protein was prone to precipitation on the affinity matrix during proteolysis. Efforts were made to optimize thrombin cleavage, including the amount of protease, temperature, time of digest and addition of detergents, but satisfactory conditions were not established. Figure 6 shows the results of attempts to elute Rac2 by thrombin cleavage. This figure also demonstrates that the glutathione elution buffer must be pH adjusted following addition of glutathione in order to elute the fusion protein from the matrix.

Due to the large amount of protein required for further analysis, a large scale purification of Rac2 and Rac2 R120E was developed. This preparation (described in the methods) was straightforward and in line with the purification described above. Three liters of cells were grown up and processed at once to generate larger quantities of protein in a more time effective manner. Protein losses were minimized by using a higher throughput protocol. Figure 7 shows the results of GST-Rac2 R120E purification by the large scale method outlined above.

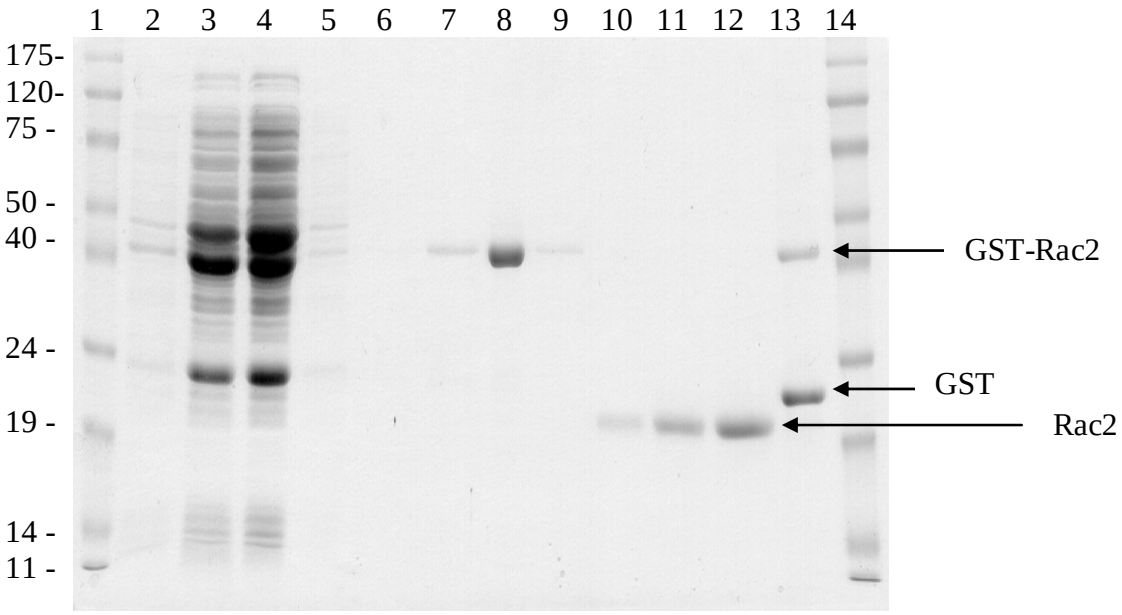

Figure 6. Optimization of GST-Rac2 purification. SDS-PAGE and Coomassie-Brilliant Blue staining was used to evaluate the various purification fractions. Loading is as follows: Lanes 1 and 14, molecular weight standards (in thousands); lane 2, whole cells; lane 3, solubilized fraction of cell lysate; lane 4, glutathione-agarose post bind; lane 5, bead wash; lane 6 and 7 are increasing concentrations of GST-Rac2 eluted with glutathione with pH unadjusted. glutathione-agarose beads after an unsuccessful elution are shown; lane 8 shows that glutathione elution buffer must be pH adjusted to ensure proper elution conditions; lane 9, bead wash following elution; lanes 10-12, Rac2 eluted directly from glutathione agarose beads by thrombin cleavage. The shift is molecular weight is due to the fact that Rac2 is no longer covalently joined to the GST fusion tag; lane 13, bead washes after thrombin elution.

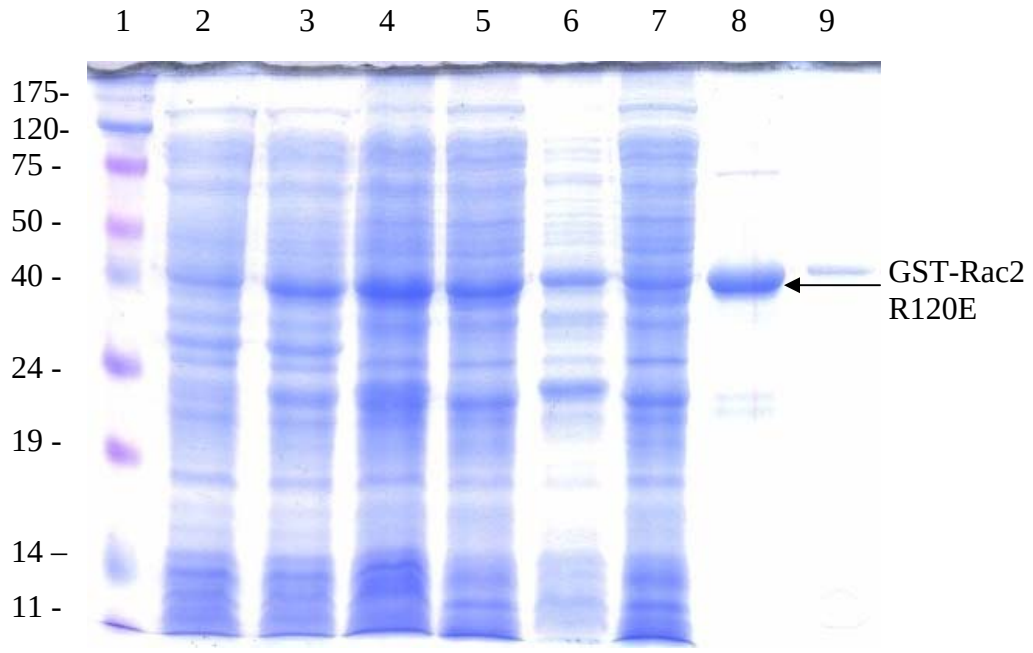

Figure 7. Large Scale Purification of GST-Rac2 R120E. SDS-PAGE and Coomassie-Brilliant Blue staining was used to evaluate the various purification fractions. Loading is as follows: lane 1, molecular weight standards (in thousands); lane 2, whole cells- pre induction; lane 3, whole cells after induction with 100 μM IPTG overnight at 18^{o}C; lane 4, lysed whole cells; lane 5, supernatant of lysed cells; lane 6, insoluble pellet of lysed cells; lane 7, flow through from glutathione agarose beads; lane 8, glutathione elution containing purified GST-Rac2 R120E; lane 9, glutathione agarose beads after elution.

Characterization of GST-Rac2 and GST-Rac2 R120E by GTPγS Binding Analysis

A key measure of Rac2 function is its ability to bind GTP. The traditional role of Rac in the cell is to act as a molecular switch and activate cell signaling when GTP bound. If Rac2 is unable to bind GTP, it will be unable to induce any of its classic downstream effectors and is rendered inactive in the cell. However, previous data demonstrating that actin binds preferentially to an "empty" Rac2 GTP binding site (Jesaitis, unpublished data), suggests that nucleotide-free Rac2 might possess interesting biological functions. To perform binding assays following purification, GST-Rac2 and GST-Rac2 R120E were

first “emptied” of guanine nucleotides by dialysis with 1 mM EDTA, which chelates metal and results in release of bound co-factor. The activity of GST-Rac2 and Rac2 R120E was then measured by a GTPγ [^{35}S] binding assay in which a radioactive nucleotide was diluted with cold nucleotide to reduce nonspecific background and allowed to bind with the isolated fusion proteins. Following incubation for various time points, unbound nucleotide was removed from nucleotide bound to GST-Rac2 by filtration. In these studies, binding specificity of GST-Rac2 was confirmed by using increasing concentrations of unlabeled nucleotide to compete with GTPγ [^{35}S] binding.

In order to fully explore the GTP binding properties of Rac2 and Rac2R120E, protocols were optimized to analyze nucleotide binding. In the following sections, all results are shown as averages of at least two experiments and error bars represent the standard deviation of the average. For these optimized studies, GST-Rac2 and GST-Rac2 R120E were purified as described previously, reagents were thawed on the day of the experiment and were kept on ice, and all reagents were subject to only one freeze/thaw cycle.

To determine if our isolated GST-Rac2 construct was binding to GTPγ [^{35}S] in a specific manner, nucleotide binding assays were conducted in the presence and absence of excess unlabeled GTP, which competes for binding with GTPγ [^{35}S]. In a typical assay, 100 pmol of Rac2 in PBS was incubated with the indicated amounts of GTPγ [^{35}S] for indicted time points. Figure 8 shows that purified GST-Rac2 binds GTP and also that GDP at a concentration of 1 mM competitively inhibited Rac2 binding to GTPγ [^{35}S]. These results show that our isolated GST-Rac2 is active and that Rac2 binds GTPγ [^{35}S]

selectively. Further calculations based on the amount of GST-Rac2 and nucleotide in the assays demonstrates that our preparations are ~80% active following purification. Error bars show SEM.

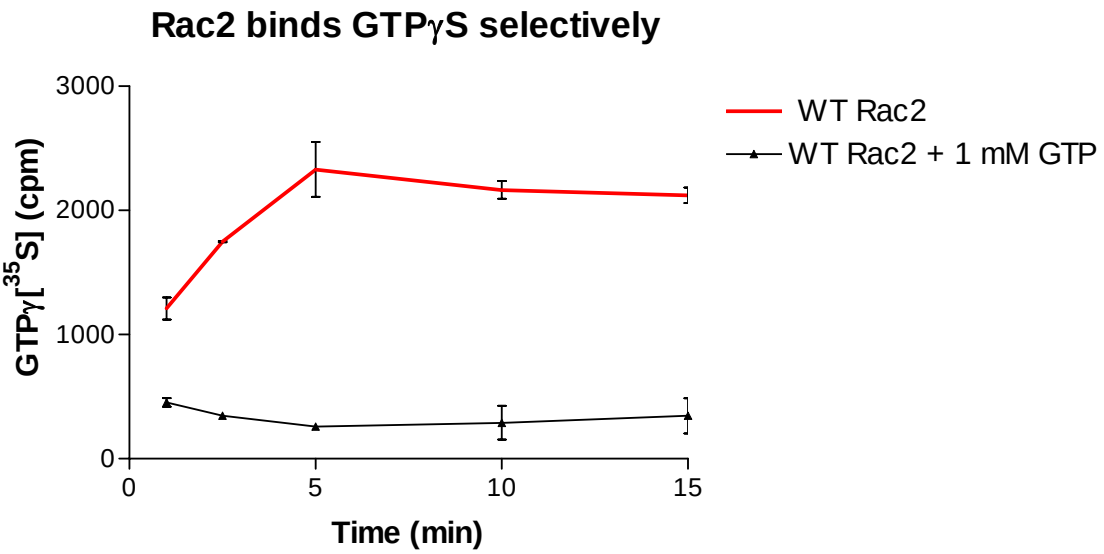

Figure 8. Nucleotide binding kinetics of purified GST-Rac2.

In contrast to GST-Rac2, GST-Rac2 R120E showed virtually no nucleotide binding under these conditions (Figure 9). The GST-Rac2 R120E mutation lies just outside the nucleotide binding site in the Rac crystal structure and appears to have a dramatic effect on binding site function. It is of interest to note that other Ras GTPases actually have an E residue at this position, and that it is unknown why this residue abolishes binding in the case of Rac2. It is also important to highlight the fact that these binding assays were conducted on GST-Rac2 samples that had been purified (with low yield) following induction with IPTG at 22^{o}. Since it was subsequently discovered that much more soluble protein was generated when cells were induced at 18^{o}C, it will be of interest to test these isolated GST-Rac2 R120E mutants in nucleotide binding assays.

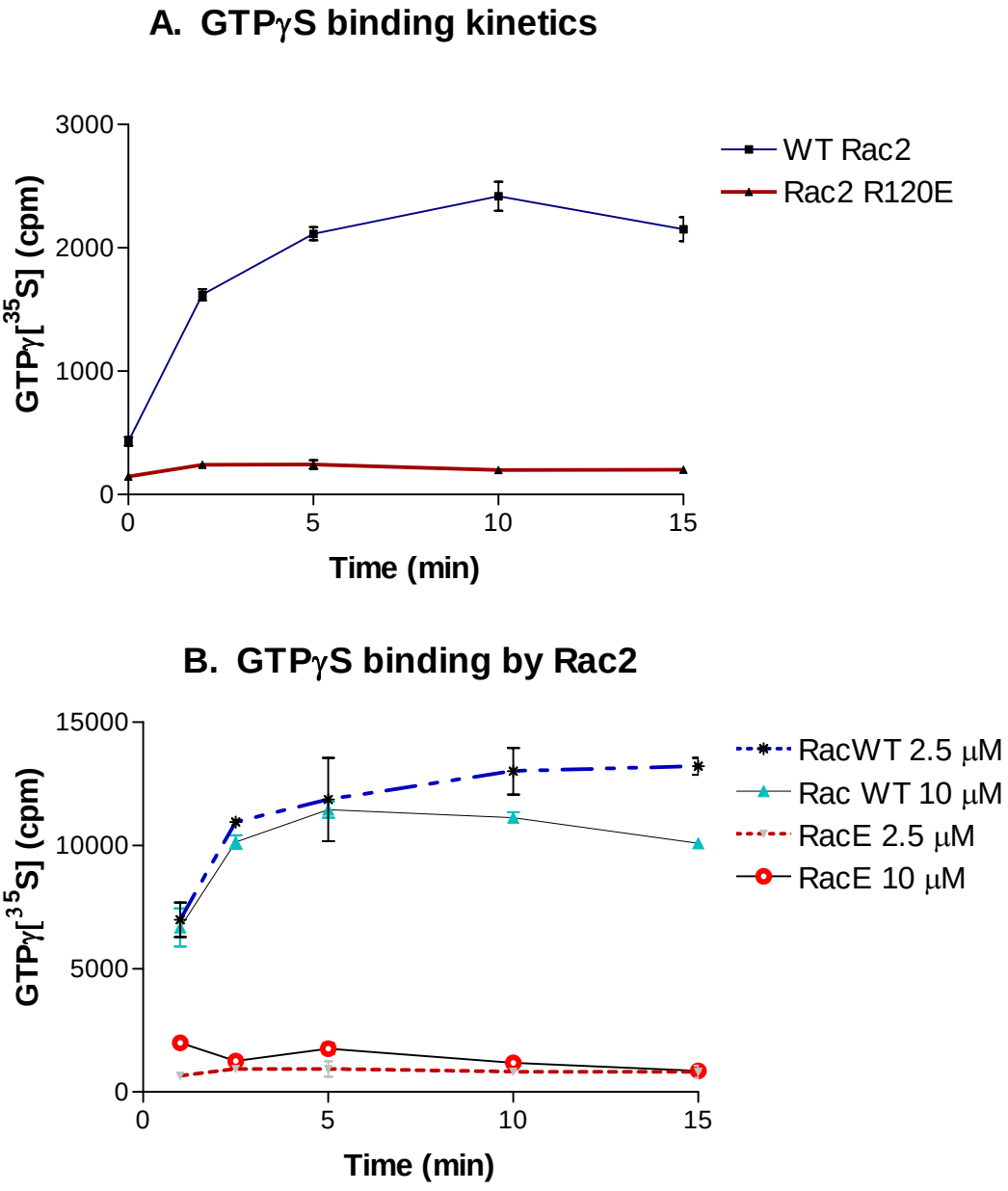

Figure 9. Rac2 and Rac2 R120E binding kinetics of GTPγS. Two representative analyses performed with different protein preparations and concentrations of nucleotide. 9A. GST-Rac2 and GST-Rac2 R120E incubated with 5 μM nucleotide. 9B. GST-Rac2 and GST-Rac2 R120E binding using 2.5 and 10 μM GTPγS with GTPγ [^{35}S]. This result suggests that Rac2 R120E doesn't bind with reduced affinity, but rather, does not efficiently bind GTP under these conditions.

Fluorescence Spectroscopy

The near UV tryptophan fluorescence emission spectrum of Rac2 and Rac2R120E was measured to examine the structural similarities of the wild type and mutant protein. Because the mutant protein, Rac2R120E, does not bind GTPγ [^{35}S] in the filtration assay, it was difficult to determine if the mutant protein had a low affinity for GTP or if the overall structure of the mutant was misfolded. Shifts in protein conformation associated with the addition of denaturing agents are measured by comparison of fluorescence emission spectrum taken under different conditions. Tryptophan fluorescence spectra can be easily measured and comparisons between wild-type proteins and mutant proteins can give evidence as to whether or not an inactive protein is misfolded (Price, 2000). Comparing spectra of native protein to denatured protein can also provide data to show that the overall protein structure is the same between GST-Rac2 and GST-Rac2 R120E.

Preliminary studies showed that 6M Guanidine caused a greater spectroscopic shift in GST-Rac2 and Rac2 R120E than denaturation by SDS. The amino acid sequences show that GST has three tryptophan residues and Rac2 has two tryptophan residues. The observed spectra represents signal from all of these residues. Since guanidine caused a much greater change in the tryptophan emission spectra, the Rac2 fusion proteins were exposed to different amounts of guanidine and fluorescence spectra was collected. As shown in Figures 10 and 11, the fluorescence peaks of GST-Rac2 and GST-Rac2 R120E are similar in the absence of guanidine and shift in a similar way in increasing guanidine. This experiment supports the hypothesis that the Rac R120E mutant has a folded conformation, but cannot bind nucleotide due to the mutation near the GTP binding site.

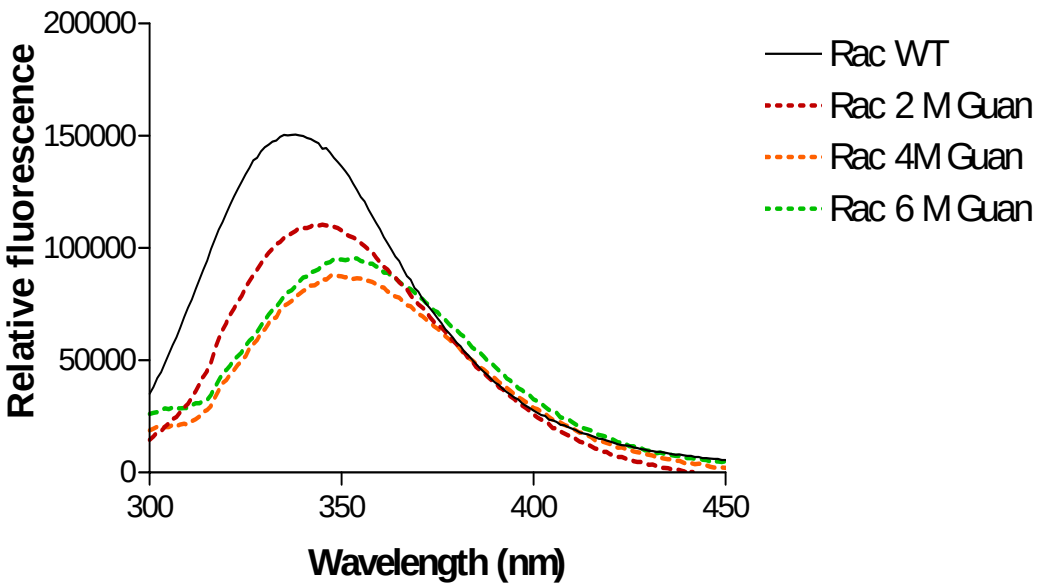

Figure 10. Denaturation of GST-Rac2 by guanidine. For these experiments, similar amount of GST-Rac2 were diluted into 0 M, 2 M, 4 M, or 6 M guanidine in PBS and incubated for 15' at room temperature. Fluorescence emission spectra were then collected using and excitation wavelength of 280 nm.

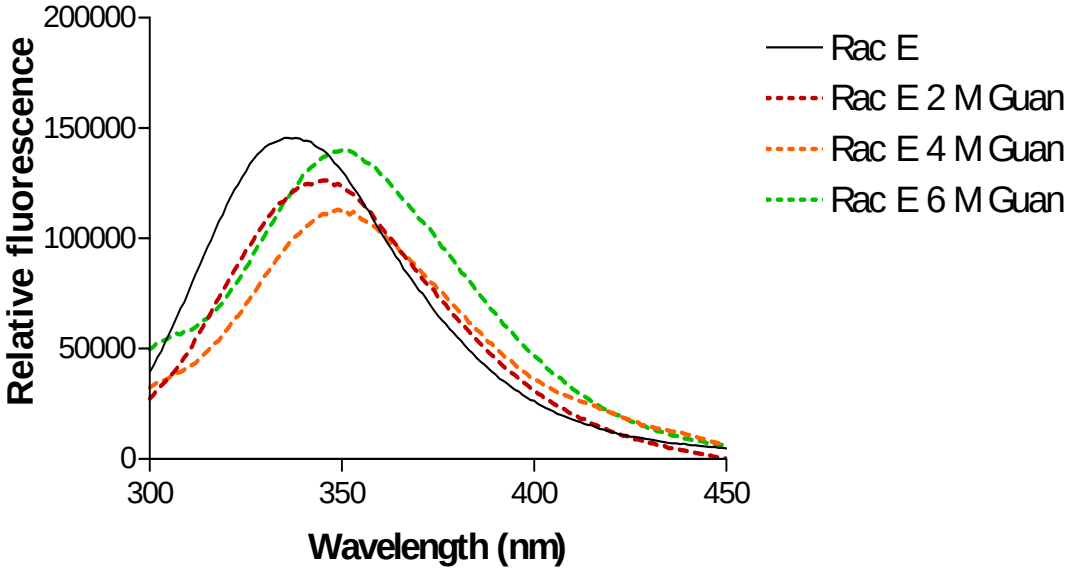

Figure 11. Denaturation of GST-Rac2 R120E by guanidine. For these experiments, similar amount of GST-Rac2 R120E were diluted into 0 M, 2 M, 4 M, or 6 M guanidine in PBS and incubated for 15' at room temperature. Fluorescence emission spectra were then collected using and excitation wavelength of 280 nm.

Phage Display

Phage display analysis has been used to map the binding epitopes of many monoclonal antibodies (Burritt, 2001, Ladner, 2004). Epitope mapping of monoclonal antibodies through phage display enables local protein structure elucidation for the antibody target protein (Bailey, 2003, Taylor, 2004). This information is of great interest when structure data about the protein in question is difficult to obtain and to provide insight into short-lived protein conformations. Due to its high specificity and extensive sequence diversity, phage display libraries are being used to isolate peptides with a high affinity for antibody and other protein targets with therapeutic value (Sidhu, 2000). In addition to the above studies, peptide mapping has been shown to produce powerful therapeutic agents with better targeting and tissue penetration than most antibodies (Ladner, 2004). Peptide mapping through phage display has also been used to characterize protein-protein binding interactions in signaling pathways (Sidhu, 2003).

The M13 phage display library is a powerful tool to analyze protein binding partners. In order to create the library used in the present studies, the phage had degenerate oligonucleotide cloned into the gene that encodes the pIII coat protein resulting in a unique nonapeptide addition to the pIII protein. A single copy of the nonapeptide is expressed at the N-terminus of each of the five pIII proteins, which increases the avidity of the peptide-binding protein interaction without compromising the bacteriophage function in a significant way. The pIII protein is required for phage infection of *E. coli*, ensuring that this protein is retained in viable phage. The distal placement of the nonapeptide relative to the phage increases the likelihood that the sequence of interest

will interact with the target protein while reducing the opportunity for the phage coat protein to bind the affinity column substrate.

The M13 phage display library J404 (a kind gift from Dr. Jim Burritt) contains $5x10^8$ unique nonapeptides and was used to determine GST-Rac2 and GST-Rac2R120E binding sequences. Various elution conditions, described previously, were employed to release phage from the GST-Rac2-Sepharose affinity columns. The overall representation of amino acids encoded by the phage has been well characterized in order to confirm that the library itself does not skew results (Burritt, 1996). This library has been shown to have a random amino acid occurrence, with only a four-fold difference between the least and most represented amino acids (cysteine and glycine, respectively).

Affinity Selected Phage Peptide Sequences

In previous studies, phage display analysis on a salt-eluted F-actin column showed a strong KXDXR sequence motif that is found in the nucleotide binding domain of some small GTP binding proteins, including Rac2 (Jesaitis, unpublished data). This result initiated the hypothesis that Rac2 might mediate actin polymerization by direct actin binding. The hypothesis was further tested by biochemical analysis of Rac-actin interactions. Synthetic peptides mimicking the F-actin binding phage consensus sequence caused up to a six fold increase in the rate of actin polymerization. In addition, slot blot analysis showed that actin bound Rac2 specifically and that this binding could be inhibited by the addition of guanyl nucleotides.

The general strategy used in our phage display experiments was to immobilize purified GST-Rac2 or GST-Rac2 R120E on CNBr-Sepharose beads to create an affinity

matrix. The J404 phage library was then allowed to interact with the column so that phage that recognize Rac2 could bind the protein column. After phage with a high affinity had bound the Rac2 column, the matrix was washed extensively to remove unbound phage. Bound phage were then eluted using a variety of conditions including 1 mM GDP, high salt and low pH. Eluted phage were then mixed with *E. coli* K91 cells and grown on solid agar in order to amplify the phage containing sequences with high affinity for GST-Rac2 or GST-Rac2 R120E. Phage titers increased by orders of magnitude after three rounds of selection, confirming the selective enrichment of phage that bound the Rac2 and Rac2 R120E affinity matrices. Phage sequences obtained for the GST-Rac2 affinity matrix following elution with GDP are shown in Table 1. In these experiments, it was hoped that GDP would specifically elute phage bound to the nucleotide binding site, which contains the KXDXR motif of Rac2.

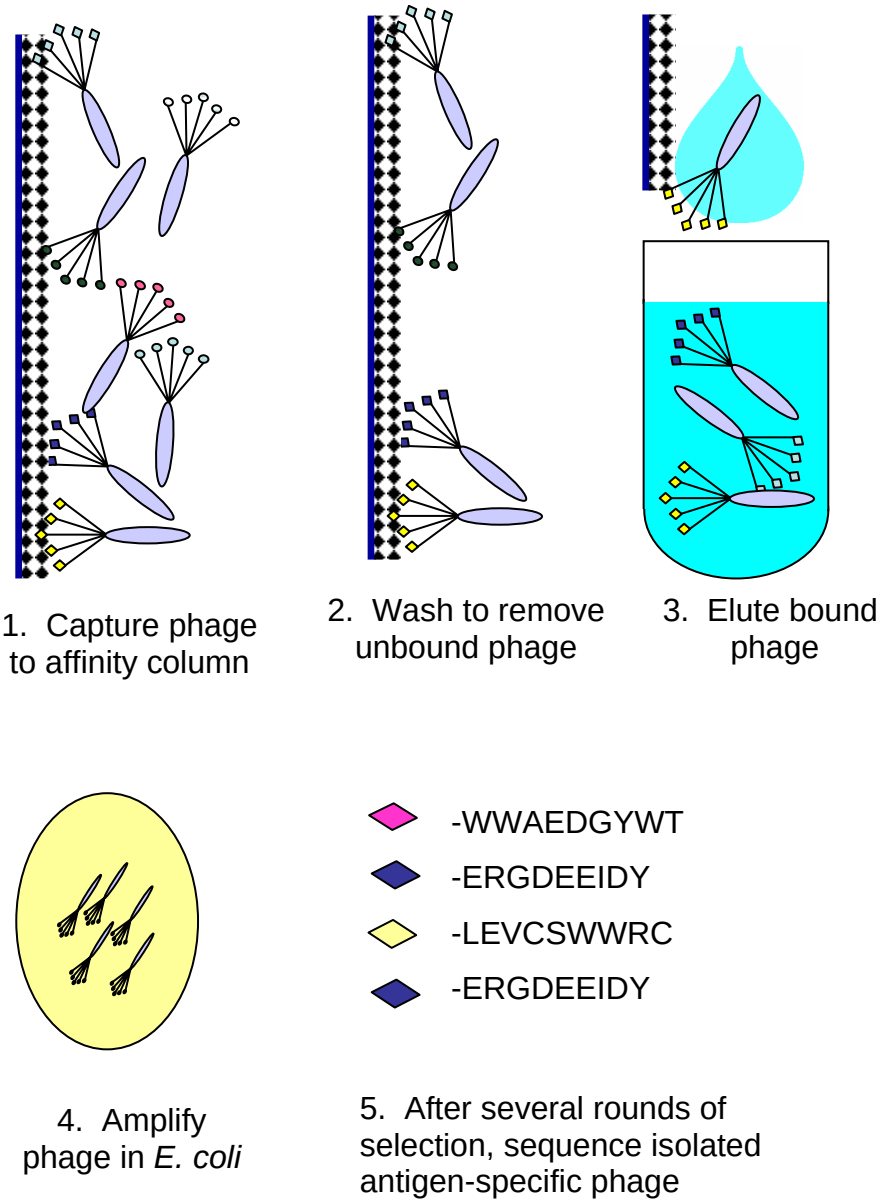

Figure 12. Phage display overview. Prior to step 1, an affinity column (in this case, GST-Rac2 or GST-Rac2 R120E) is generated. A phage library is incubated on the columns (1), unbound phage are removed (2), adherent phage are eluted (3), and phage are amplified in *E. coli*. After selection is complete, isolated phage are sequenced to determine the peptide sequence with high affinity for the protein column.

ASKGMAPPV	RGYEFRNPA	GLTPDWMSG	NLVKFATLL
QEVKEMSTA	SWTGWPPVG	PAFWEEENK	LAKHWDDRW
MDGLSMFFH	TNGQASPPQ	RDLVVNPVS	SQVGKLEPE
VKYPGIFAG	ENIWLMPHP	LASRVLTMG	NAGLPVYSV
ERVVGMDGQ	LSTKGGVGK	RLGAQARPT	SNQNEVPQG
EGWMKPSWP	EWMIGSQEM	PNMPTLWSL	TDSGKQVEK
ANSGVSGLP	RTLDIKRAF	LIMEQDRNE	GGDNGLNTP
KQDGELGSA	TYLDNDKLG	GFPRPEVLG	VKHVQNRDA
VSDVKGQKH	VGRFDSKPV	DWWLSGTQS	LTNIALGHL
KVWDPGLFR	EGGHTFHWL	KILNVDSSG	WTKSAWGSA
RLDSSSARD	KISMLRKLD	GIGVSYERR	VWADINQYW
VPRLAGGPV	QLRFVHKMA	WDIVKRLQP	FSFRLEDHW
GQIQRWAKK	NTVKRFMFG	QDVATDSRV	DVHGFLKRA
WIDVRSSHA	QFVVEHHSM	SARYSQEQW	PEMGHGATK
YGYTVNLNA	WGIMSLSTM	APMHWYQSG	EWMIGSQEM
AAAFYSHGV	FLKDSPMGG	RGDMGGAYS	RRQATERKA
WPFFQAPQN	VTKLQGRDK	GFDWNRKKA	GGFKAFAQR
NWPYRWDVP	TLGAQHDRN	WGPTGANRL	GYPSKSHLG
VKVKWADRL	GMLGSRNAM	GYSWLQTNH	VLNMAYPQR
TGLLNKRKA	AHHTGWMQN	DLFWPARSV	AQWKYHLIG

Table 1. Peptide sequences from phage display selected on the GST-Rac2 affinity matrix eluted with GDP. Following binding and column washing, phage were eluted from the GST-Rac2 beads using 1 mM GDP. Eighty full-length peptides were sequenced after the third round of amplification.

In a similar set of experiments, phage display was conducted on a GST-Rac2 R120E affinity matrix, since the R120E mutation has been shown to enhance actin binding in slot blot assays (Jesaitis, unpublished data). Phage peptide sequences obtained from phage display using three different elution conditions for GST-Rac2 R120E are shown in Table 2. A strong consensus sequence was identified between phage eluted from the R120E mutant under high salt (2 M NaCl) and low pH (0.1 M glycine, pH 2.2) conditions, many sequences from these elutions were identical.

GST-Rac2 R120E 1 mM GDP Elution	GST-Rac2 R120E High Salt Elution	GST-Rac2 R120E Low pH Elution
GKLSLLPTG	ERGDEEIDY	ERGDDWELE
EYRNYDRRL	WWAEDGYWT	ERGDDWELE
GVMLTHRLG	ERGDDWELE	WWAEDGYWT
VKWGSDSAS	ERGDEEIDY	WWAEDGYWT
NRAVDHLRG	WWAEDGYWT	WWAEDGYWT
AGKLSIERL	SIVHTLSRA	WWAEDGYWT
SAGFKGMDR	ERGDEEIDY	ERGDDWELE
NDFTRQHRG	ERGDDWELE	WWAEDGYWT
GSWDVMVET	ERGDEEIDY	WWAEDGYWT
GTLHLA	ERGDDWELE	ERGDDWELE
ATQHERRSA	ERGDDWELE	MQGILRDNP
VGSKTTGGS	WWAEDGYWT	WWAEDGYWT
KGITRAVED	ERGDEEIDY	WWAEDGYWT
IEATGKVPV	ERGDEEIDY	WWAEDGYWT
ADIKIKWHG	ERGDEEIDY	ERGDDWELE
KVNNSRPND	ERGDEEIDY	ERGDDWELE
GPWEIISFA	ERGDDWELE	
NHKPVGRAP	LEVCSWWRC	
GIAYVTHQH	ERGDDWELE	
WGWGALGPL	WWAEDGYWT	
NKISLKRPP	ERGDEEIDY	
	ERGDDWELE	
	ERGDEEIDY	
	ERGDEEIDY	

Table 2. GST-Rac2 R120E phage sequences from three elution conditions. Following binding and column washing, phage were eluted with either 1 mM GDP, 2 M NaCl or pH 2.2. Many of the phage sequences eluted with high salt and low pH are identical, suggesting strong positive selection.

Phage DNA Sequence Analysis using FINDMAP

FINDMAP and EPIMAP, an updated version, are a computer programs designed to predict three dimensional binding epitopes by comparing the amino acid probe sequences (selected phage) against the amino acid sequence of a target protein. The program is designed to predict discontinuous epitope regions that form a protein-protein interaction site by permitting large gaps in the target sequence (actin in the present study) during

alignment and by ignoring sequence direction. FINDMAP was developed at Montana State University and was first reported by Mumey et al, 2003 and Bailey et al., 2003 and has been shown to identify surface accessible binding regions using nearest neighbor mapping.

Using the program FINDMAP, phage eluted from GST-Rac2 or GST-Rac2 R120E columns using 1 mM GDP did not show a very strong consensus alignment with regions found in the actin amino acid sequence (Figure 13). This result could be due to the complex nature of the GDP binding pocket, creating a site that binds a diverse array of phage or simply from selection of a diverse array of phage that have substantial affinity for GDP.

The results from analysis of eighty full length phage sequences selected on the Rac2 affinity matrix are shown in Figure 13. Analysis of the phage sequences obtained from Rac2 R120E using either GDP or high salt are shown in Figure 14 and 15, respectively. A comparison of the FINDMAP results from all three experiments is shown in Figure 16. The regions showing the greatest frequency in this histogram were modeled onto the three dimensional surface of actin as described in the following section.

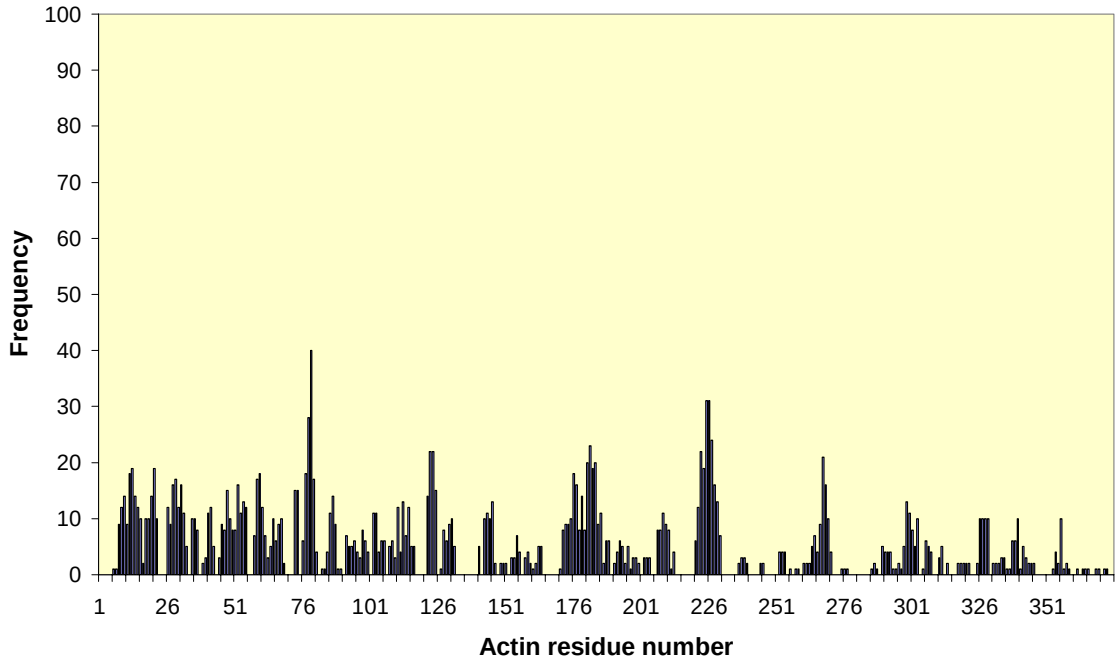

Figure 13. FINDMAP analysis of phage eluted from GST-Rac2 with 1 mM GDP. This histogram shows the frequency of phage residue assignment on the human actin target that may form a putative Rac2 binding site.

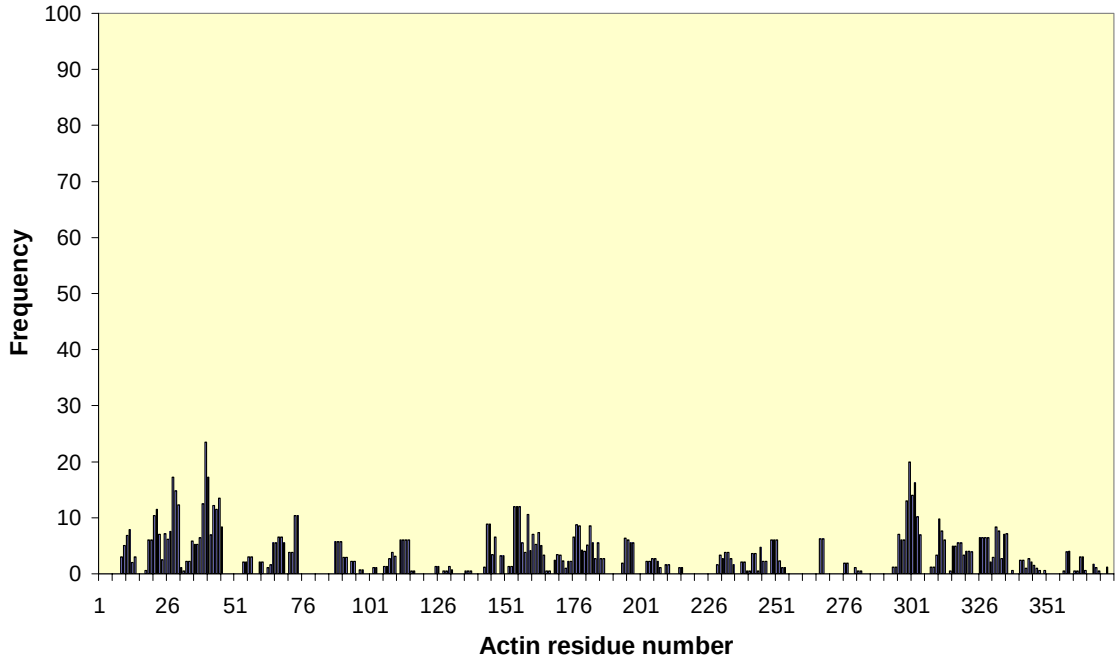

Figure 14. FINDMAP analysis of phage eluted from GST-Rac2 R120E with 1 mM GDP. This histogram shows the frequency of phage residue assignment of the human actin target that may form a putative Rac2 R120E binding site.

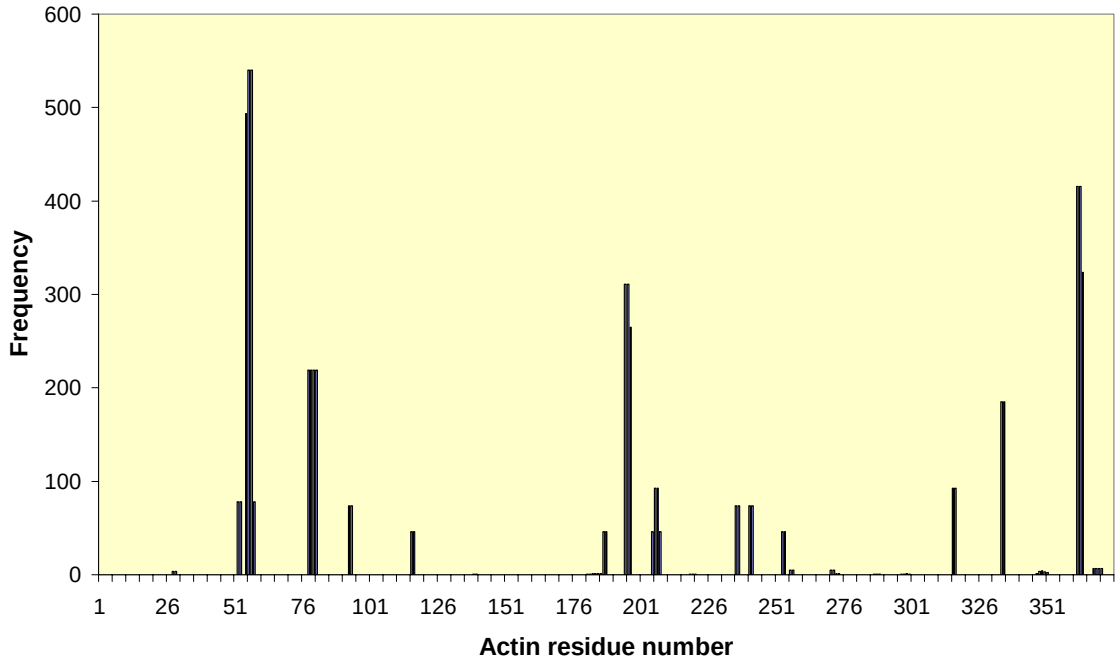

Figure 15. FINDMAP analysis of phage eluted from GST-Rac2 R120E with high salt. This histogram shows the frequency of phage residue assignment on the human actin target that may form a putative Rac2 binding site.

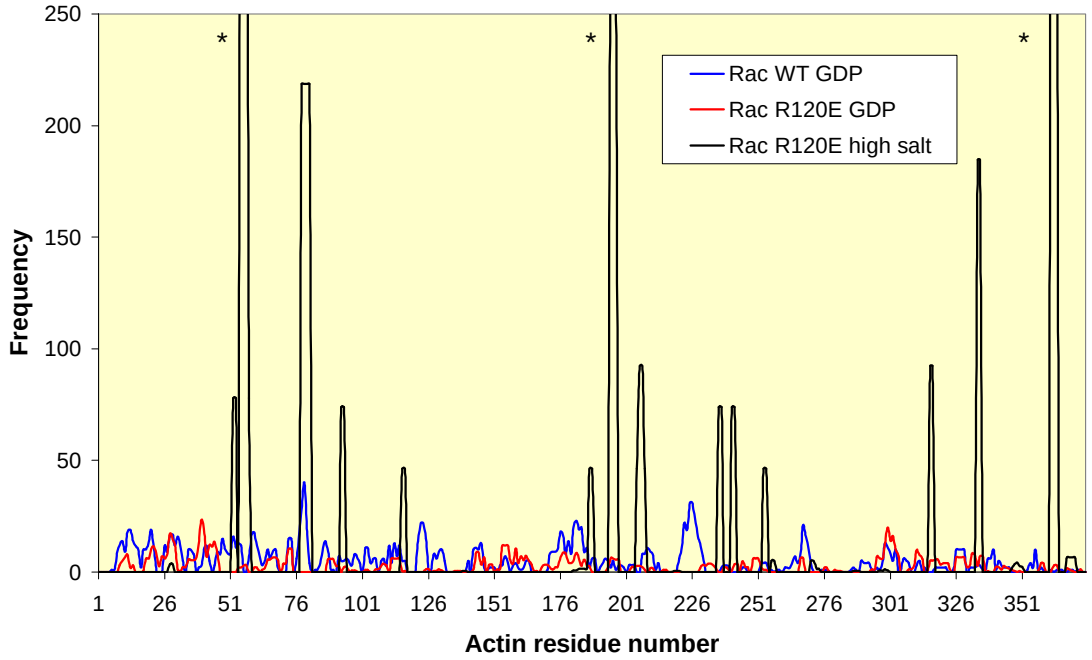

Figure 16. Comparison of FINDMAP analysis frequency results. This graph shows the frequency of phage residue assignment on the human actin target sequence. (*) indicates that the frequency of the residue is greater than 250.

Visualizing the FINDMAP results on the three dimensional surface of actin

The program Swiss PDB viewer is a publicly available protein modeling program for protein structure, and serves as a "sequence to structure workbench and viewing program" (Schwede, 2000) where a user can begin with a known protein structure and make mutations in selected amino acid residues. Swiss PDB Viewer and Swiss MODEL, a companion internet-based server for automated comparative protein modeling, are available over the World Wide Web at: http://www.expasy.org/spdbv/ (Guex, 1997). This program, released in 1993, pioneered the computer based protein modeling field and continues to be the most widely used publicly available protein modeling software.

Using a computer model of human beta actin, we are able to approximate the surface accessibility and proximity of the phage binding sequence on the actin model. The crystal structure of human actin has not yet been solved, but the structure of rabbit actin is known (Klenchin, 2003). Human and rabbit actin are very similar and share 93% amino acid identity as shown in Figure 17. To assess results obtained with FINDMAP, Swiss PDB Viewer was used to map the surface of human actin. This crystal structure of monomeric actin was solved in complex with jaspisamide A and kabiramide C, both trisoxazole macrolide toxins produced by marine sponges (Klenchin, 2003). Actin has previously been crystallized in complex with other actin-capping proteins with very consistent results, showing that these toxins do not cause a significant conformational shift. Considering the highly conserved structure of actin, 24 out of 375 amino acids were mutated to convert the structure of rabbit actin (PDB file 1QZ6) to that of human actin.

A.

```
MDDDIAALVVDNGSGMCKAGFAGDDAPRAVFPSIVGRPRHQGVMVGMGQKDSYVGDEAQS
DEDETTALVCDNGSGLVKAGFAGDDAPRAVFPSIVGRPRHQGVMVGMGQKDSYVGDEAQS
 :*: :*** ***** :****************************************

KRGILTLKYPIEHGIVTNWDDMEKIWHHTFYNELRVAPEEHPVLLTEAPLNPKANREKMT
KRGILTLKYPIEHGIITNWDDMEKIWHHTFYNELRVAPEEHPTLLTEAPLNPKANREKMT
***************:*************************.*****************

QIMFETFNTPAMYVAIQAVLSLYASGRTTGIVMDSGDGVTHTVPIYEGYALPHAILRLDL
QIMFETFNVPAMYVAIQAVLSLYASGRTTGIVLDSGDGVTHNVPIYEGYALPHAIMRLDL
********.***********************:********.*************:****

AGRDLTDYLMKILTERGYSFTTTAEREIVRDIKEKLCYVALDFEQEMATAASSSSLEKSY
AGRDLTDYLMKILTERGYSFVTTAEREIVRDIKEKLCYVALDFENEMATAASSSSLEKSY
********************.***********************:***************

ELPDGQVITIGNERFRCPEALFQPSFLGMESCGIHETTFNSIMKCDVDIRKDLYANTVLS
ELPDGQVITIGNERFRCPETLFQPSFIGMESAGIHETTYNSIMKCDIDIRKDLYANNVMS
********************:******:****.******:*******:*********.*:*

GGTTMYPGIADRMQKEITALAPSTMKIKIIAPPERKYSVWIGGSILASLSTFQQMWISKQ
GGTTMYPGIADRMQKEITALAPSTMKIKIIAPPERKYSVWIGGSILASLSTFQQMWITKQ
************************************************************:**

EYDESGPSIVHRKCF
EYDEAGPSIVHRKCF
****:**********
```

B.

```
1   MDDDIAALVVDNGSGMCKAGFAGDDAPRAVFPSIVGRPRHQGVMVGMGQKDSYVGDEAQS
61  KRGILTLKYPIEHGIVTNWDDMEKIWHHTFYNELRVAPEEHPVLLTEAPLNPKANREKMT
121 QIMFETFNTPAMYVAIQAVLSLYASGRTTGIVMDSGDGVTHTVPIYEGYALPHAILRLDL
181 AGRDLTDYLMKILTERGYSFTTTAEREIVRDIKEKLCYVALDFEQEMATAASSSSLEKSY
241 ELPDGQVITIGNERFRCPEALFQPSFLGMESCGIHETTFNSIMKCDVDIRKDLYANTVLS
301 GGTTMYPGIADRMQKEITALAPSTMKIKIIAPPERKYSVWIGGSILASLSTFQQMWISKQ
361 EYDESGPSIVHRKCF
```

Figure 17. Actin amino acid sequence analysis. A, Clustal W alignment of human beta actin and rabbit skeletal actin. Human actin NCBI accession number 12803203 rabbit actin NCBI accession number 71611. B, FINDMAP results from phage eluted from GST-Rac2 R120E with high salt shown on the human actin sequence. Underlined sequence regions are identical to eluted phage sequence. Colors represent frequency of FINDMAP hits: yellow, +400; green, 150-400; pink, 45-150.

FINDMAP results from phage eluted from GST-Rac2 R120E are shown on the primary sequence of actin in Figure 17B. Some identified epitopes that are in close proximity in the actin 3D structure are actually far apart in the primary amino acid sequence. For example, amino acid residues 55 and 56 are adjacent to residues 205-208 in the 3D model.

Swiss PDB viewer was then used to view the human actin model, as shown in Figure 18. Panel 18a shows a space filling model of a human actin monomer in two different orientations, a side-ways view and a top-down view color coded to show surface accessibility in an aqueous environment. In the report of this structure, the authors compared the actin structures generated with the two toxins bound and found that the few substantial shifts between the structures were in intrinsically flexible regions between residues 53-67, 199-208 and, 238-248 (Klenchin, 2003). It is interesting that these regions are identified as being flexible, as they overlap with some of the FINDMAP results for Rac2 R120E eluted with high salt, as shown in Figure 18b and 18c. Space filling actin monomers are shown with amino acids colored from most to least selected by FINDMAP as follows: yellow: residues 55-57 and 362-364; green: 78-81, 195-197, 334-335; pink, 52-53, 93-94, 116-117, 187-188, 205-208, 236-237, 241-242, 253-254, 316-317.

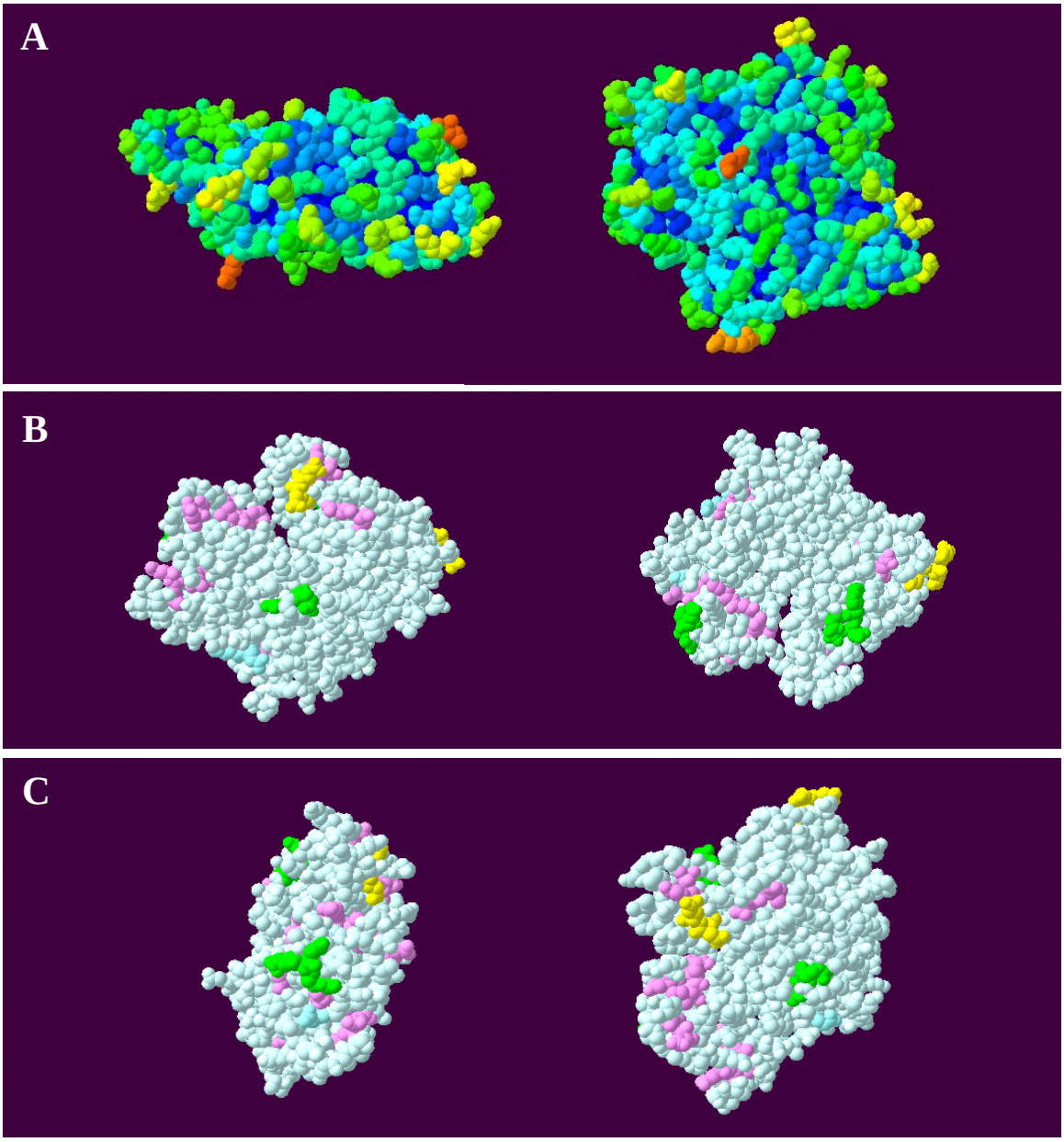

Figure 18. Space filling model of human actin monomers. A, side and top views (90^{o} rotation on a horizontal axis) of actin showing surface accessibility in an aqueous environment. Warmer colored residues are the most accessible, while cooler colored residues are more buried. B, top and bottom views (180^{o} rotation) of actin with amino acids identified by FINDMAP labeled as follows: yellow: residues 55-57 and 362-364; green: 78-81, 195-197, 334-335; pink, 52-53, 93-94, 116-117, 187-188, 205-208, 236-237, 241-242, 253-254, 316-317. C, actin monomers rotated approximately 45^{o} to best show regions with possible Rac2 docking sites.

Because actin exists in both a monomeric and filamentous state, it is important to consider potential binding epitopes and constraints caused by polymerization. The crystal structure of filamentous actin has not been solved because when actin polymerizes, it forms filaments of variable length, which do not pack uniformly enough to form crystals suitable for structure determination. The structure of an actin trimer complexed with gelsolin-1 has been determined to 2.2 Å, and was used to generate an F-actin trimer model (Dawson, 2003).

The actin trimer was used to investigate potential Rac2 binding epitopes formed when the surfaces of different actin monomers contact each other as shown in Figure 19. In this figure set, an actin trimer is shown with the axis of polymerization lying horizontal to the frame. The three monomers are shown in red, green and blue, respectively. Residues frequently selected by FINDMAP are shown in yellow on all three monomers. The orientation of the trimer is identical in all three frames: 19A shows a stick model of an actin trimer, including all side chains; 19B, a space filling representation of the previous image; 19C, an enlargement of 19B to show the contact regions between the three actin monomers in greater detail. The PDB actin models of FINDMAP data certainly suggest that severa; possible binding sites, including ones utilizing more than one set of identified residues, may exist for Rac2 and ongoing studies are analyzing this possibility in greater detail.

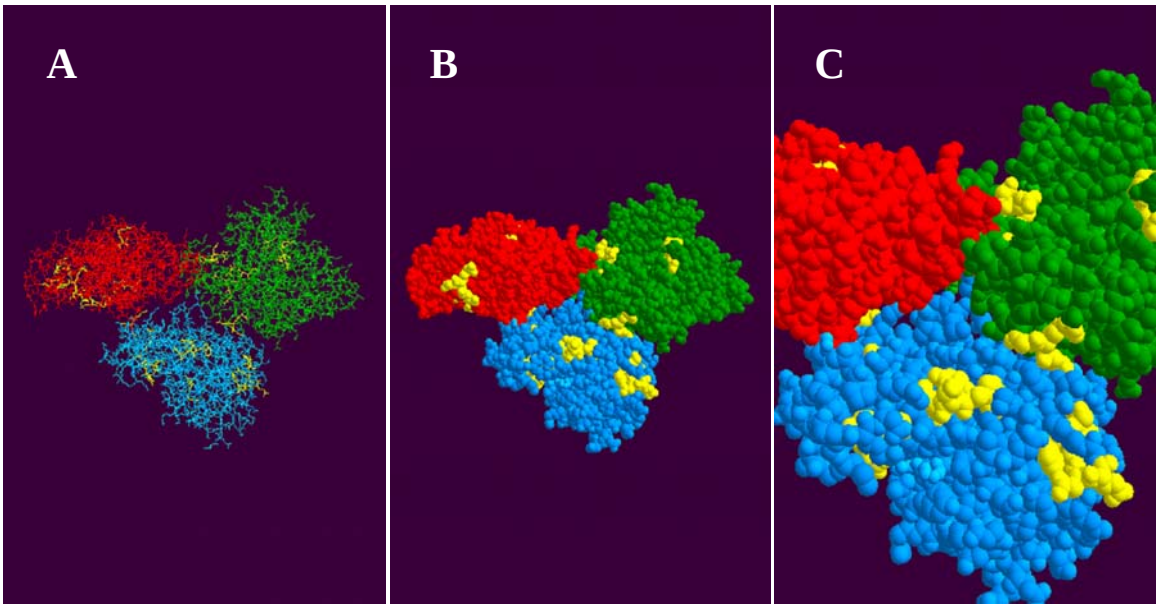

Figure 19. Actin trimer highlighting residues frequently identified by FINDMAP. A, stick model of an actin trimer, including all side chains; B, a space filling representation; C, an enlargement showing the contact regions between the three actin monomers in greater detail.

Expression of Rac2 and Rac2 R120E in a Mammalian Cell Line

Fluorescence microscopy is an elegant technique for assaying protein function and localization in cell culture systems. Mammalian cell lines have the correct machinery to add post-translation modifications and are well-suited to express mammalian proteins to evaluate biological functions. Adherent mammalian cells can be grown on coverslips and immuno-stained with a fluorescently conjugated secondary antibody for microscopy, or proteins of interest can be tagged with a specific recognizable protein or peptide to analyze the effects of heterologously expressed proteins. For preliminary studies outlined in this section, constructs were generated for the regulated, overexpression of human Rac2 and Rac2 R120E in a human cell line. The ultimate goal of these ongoing studies

will be to use immunofluorescence microscopy to evaluate any effects of the R120E mutation on actin dynamics in living cells.

Inducible Protein Production using GeneSwitch Vectors

The GeneSwitch transfection system is a mifepristone-inducible protein expression system that is tightly regulated through a combination of yeast and human transcription factors. Successful protein production using the two GeneSwitch plasmids, pGene and pSwitch, has been reported in the literature by several groups (Oram 2001, Yan 2003, Akimov 2003). In the present work, we transfected human embryonic kidney (HEK) cells to examine the GeneSwitch cell expression system as a platform for the inducible expression of Rac2 and Rac2 R120E. The HEK cell line used had already been stably transfected with the pSwitch vector, which could be selected for using hygromycin b, and was transfected to include pGene Rac2 and Rac2 R120E using Lipofectamine 2000. The Rac2 gene used was derived from the pGEX GST-Rac2 and R120E mutant as described previously by restriction digests and was cloned into the pGene vector for mammalian expression.

An additional set of constructs that were generated include the addition of a c-myc tag, to aid in the identification of overexpressed Rac2 compared to other cellular Rac isoforms. The c-myc tag sequence (kindly provided by Dr. Heini Miettien), was incorporated into either the amino or carboxyl termini of the Rac2 forms by PCR mutagenesis. The carboxyl terminus of Rac2 is critical for proper membrane localization, and mutations to this region can cause Rac2 to be inactive. For this reason, preliminary studies have focused on the Rac N-terminal myc tag construct. The general scheme for

generating the various pGene Rac constructs is shown in Figure 20 and the confirmed amino acid sequences of the pGene Rac2 N-terminal myc tag constructs are shown in Figure 21.

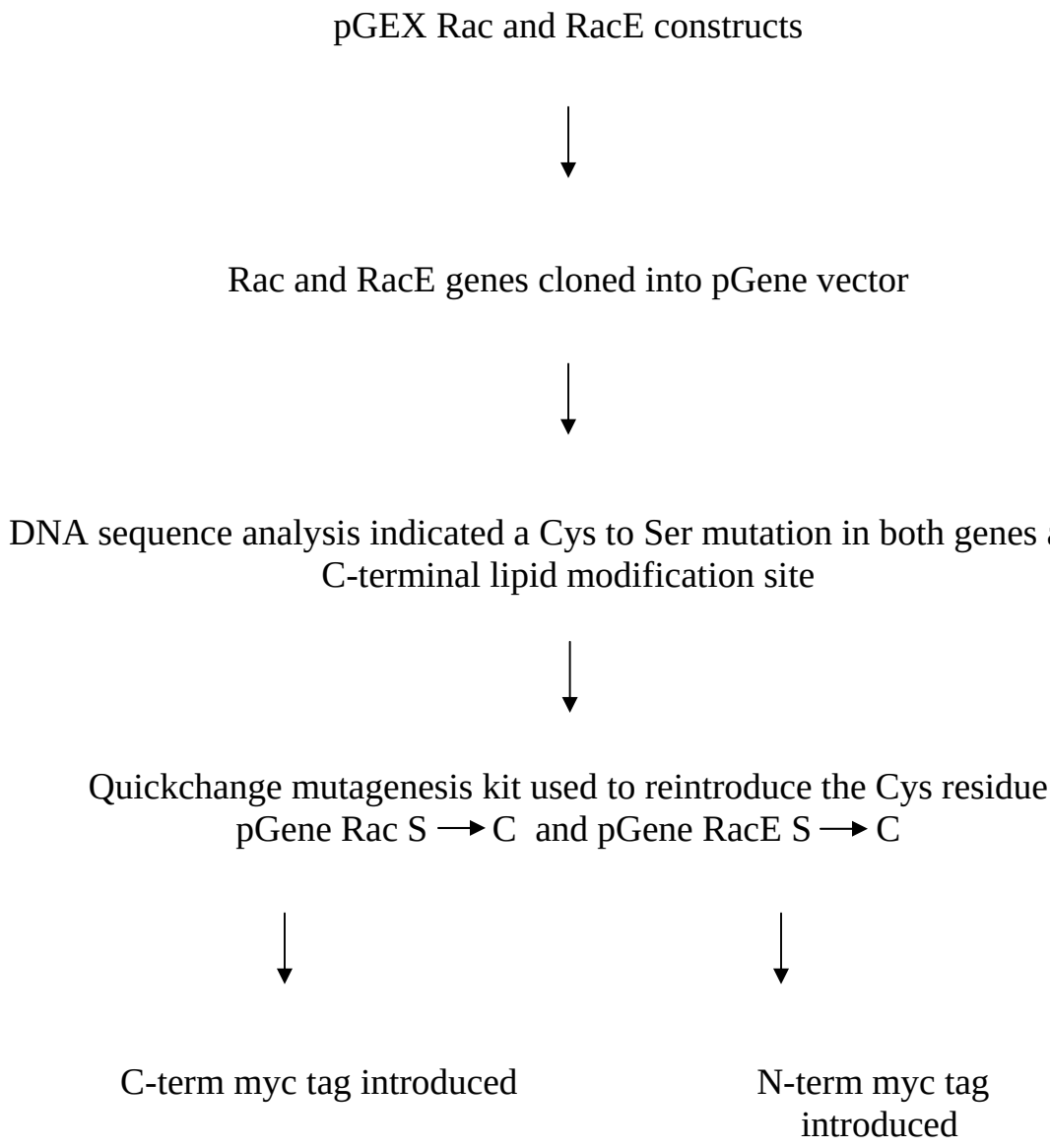

Figure 20. Overview of methods used to generate Rac2 mammalian expression constructs.

Sequence analysis of N-term myc constructs (tag shown in bold)

```
Myc-Rac2,
1 MEQKLISEEDLQAIKCVVVGDGAVGKTCLLISYTTNAFPGEYIPTVFDNYSANVMVDSKP
Myc-Rac2E,
1 MEQKLISEEDLQAIKCVVVGDGAVGKTCLLISYTTNAFPGEYIPTVFDNYSANVMVDSKP
  ************************************************************

Myc-Rac2,
61 VNLGLWDTAGQEDYDRLRPLSYPQTDVFLICFSLVSPASYENVRAKWFPEVRHHCPSTPI
Myc-Rac2E,
61 VNLGLWDTAGQEDYDRLRPLSYPQTDVFLICFSLVSPASYENVRAKWFPEVRHHCPSTPI
   ************************************************************

Myc-Rac2,
121 ILVGTKLDLRDDKDTIEKLKEKKLAPITYPQGLALAKEIDSVKYLECSALTQRGLKTVFD
Myc-Rac2E,
121 ILVGTKLDLEDDKDTIEKLKEKKLAPITYPQGLALAKEIDSVKYLECSALTQRGLKTVFD
    ********* ************************************************

Myc-Rac2,    181 EAIRAVLCPQPTRQQKRACSLL
Myc-Rac2E,   181 EAIRAVLCPQPTRQQKRACSLL
             **********************
```

Figure 21. Protein sequence alignment of pGene Rac2 and pGene Rac2 R120E constructs with an N-terminal c-myc tag. The c-myc tag is shown in the blue box and the Rac2 R120E mutation is highlighted by the orange box.

For preliminary studies, cells were transiently transfected, meaning that selection with antibiotics was not used to isolate cells expressing the plasmid of interest. Twenty four hours after transfection, cells were induced with 10 ng/ml Mifepristione for another twenty four hours. Because HEK cells do not always adhere to glass surfaces strongly enough for long staining procedures, and the use of poly-l-lysine treated coverslips was important to improve adherence. For this early study, cells were stained with mAb 9E10, a commonly used antibody directed against the amino terminal c-myc tag. Preliminary data suggests that GST-Rac2 and R120E are inducibly expressed and are indeed localized to the cell membranes. HEK cells transiently transfected with pGene myc Rac2, pGene myc Rac2 R120E, or LacZ pGene, a control vector used to assay for transfection efficiency, are shown in Figure 22. It is of interest to note that after immunofluorescent

staining, only HEK cells transformed with the pGene myc Rac2 vectors showed and significant fluorescence. The images of cells transformed with LacZ were overexposed to allow the fluorescence background.

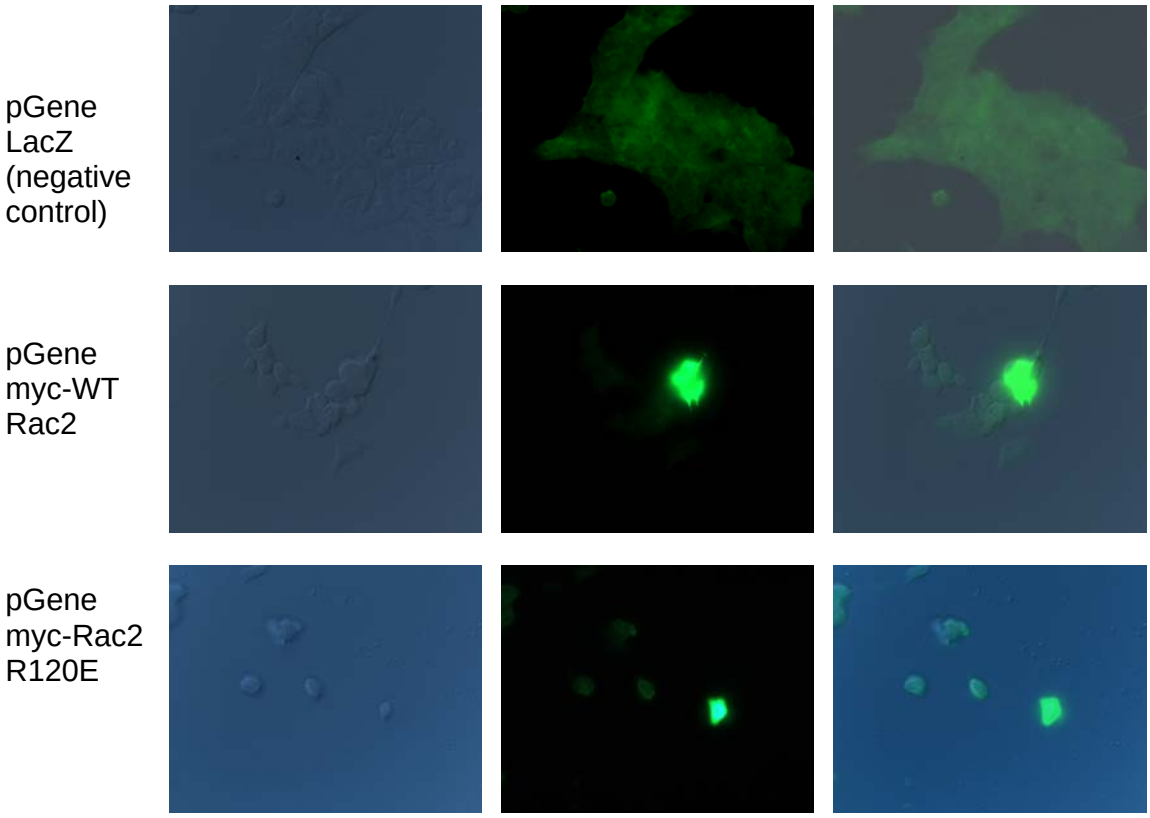

Figure 22. Immunofluorescence of HEK cells transiently transfected with pGene c-myc Rac2, c-myc Rac2 R120E or LacZ. Cells were induced for 24 hours with mifepristone and stained with the α-Myc antibody 9E10.

In future studies, it might be of interest to use CHO cells rather than HEK cells since CHO cells have substantially higher transfection efficiencies and adhere to glass coverslips much more tightly than HEK cells. CHO cells have also been extensively studies using immunofluorescence to characterize the actin cytoskeleton. Finally, stable

cell lines transfected with wild-type and mutant forms of the seven transmembrane human N-formyl peptide receptors that confer sensitivity to fMLF chemotactic peptides are also available should Rac2 transfection prove to be of physiological interest.

CHAPTER FOUR

CONCLUSIONS

The Rac proteins are key regulators of many diverse cellular functions through their effects on cytoskeletal organization. Rac2 is a small GTP binding protein involved in regulating many cellular activities, especially those directed by actin cytoskeletal rearrangements. In different cellular locations, Rac activates pathways in many tissues that are important in cell physiology, including actin remodeling, motility, gene expression, and cell cycle progression and has been shown to cause tumorigenesis under the right conditions. In human neutrophils, Rac2 is involved in the NADPH oxidase complex, a critical pathway for host defense through the generation of reactive oxygen species. The primary purpose of our studies was to examine the hypothesis that Rac2 binds directly to actin, affecting the regulation of actin polymerization. A different small GTP binding protein, Rap2, has been shown to interact with actin through direct binding.

To this end, we purified and characterized GST-Rac2 and GST-Rac2 R120E from *E.coli* and used phage display mapping to identify potential binding sites on actin. Purified GST-Rac2 and GST-Rac2 R120E were extensively characterized to show that purified protein was free from contamination. The GTP binding activity of both GST-Rac2 and GST-Rac2 R120E were determined using a GTPγ [^{35}S] binding assay. GST-Rac2 was shown to bind GTPγ [^{35}S] selectively, but GST-Rac2 R120E did not bind GTPγ [^{35}S]. Fluorescence spectroscopy results suggested that the structural conformation of the purified wild type and mutant protein were similar.

Phage display analysis, which has been used to map binding epitopes on other proteins, was conducted on GST-Rac2 and GST-Rac2 R120E affinity matrices using the phage library J404. Peptide sequences from phage display on both proteins were mapped to the amino acid sequence of human actin using the program FINDMAP. This program can identify discontinuous protein binding sites regions by performing alighnments of amino acid residues irrespective of sequence direction and by permitting large gaps in the target sequence during alignment. FINDMAP results were visualized using Swiss PDB Viewer, a publicly available protein modeling program and workbench. Several possible binding epitopes for Rac2 were identified on the surface of actin that would be available for binding to polymerized actin.

In addition to the purification of recombinant protein expressed in *E. coli*, we generated vectors to express c-myc tagged Rac2 and Rac2 R120E in mammalian cell lines. Mammalian cell lines are well-suited to evaluate biological functions and protein localization of mammalian proteins. Preliminary fluorescence microscopy data shows that indeed c-myc tagged Rac2 and Rac2 R120E are expressed using the GeneSwitch inducible transfection system. Future studies will determine the effect of Rac2 R120E on the actin cytoskeleton in mammalian cells, confirming Rac2 binding to actin by inhibition using actin-identified peptides, and search for possible other protein binding sites by application of FINDMAP to sequences of known Rac-binding proteins.

REFERENCES CITED

D. Abdel-Latif, M. Steward, D. L. Macdonald, G. A. Francis, M. C. Dinauer, and P. Lacy. Rac2 is critical for neutrophil primary granule exocytosis. *Blood* 104 (3):832-839, 2004.

S. S. Akimov and A. M. Belkin. Opposing roles of Ras/Raf oncogenes and the MEK1/ERK signaling module in regulation of expression and adhesive function of surface transglutaminase. *J.Biol.Chem.* 278 (37):35609-35619, 2003.

B. W. Bailey, B. Mumey, P. A. Hargrave, A. Arendt, O. P. Ernst, K. P. Hofmann, P. R. Callis, J. B. Burritt, A. J. Jesaitis, and E. A. Dratz. Constraints on the conformation of the cytoplasmic face of dark-adapted and light-excited rhodopsin inferred from antirhodopsin antibody imprints. *Protein Sci.* 12 (11):2453-2475, 2003.

R. Begum, E. Kamal MS Nur, and M. A. Zaman. The role of Rho GTPases in the regulation of the rearrangement of actin cytoskeleton and cell movement. *Exp.Mol.Med.* 36 (4):358-366, 2004.

S. Blankenberg, S. Barbaux, and L. Tiret. Adhesion molecules and atherosclerosis. *Atherosclerosis* 170 (2):191-203, 2003.

V. Brinkmann, U. Reichard, C. Goosmann, B. Fauler, Y. Uhlemann, D. S. Weiss, Y. Weinrauch, and A. Zychlinsky. Neutrophil extracellular traps kill bacteria. *Science* 303 (5663):1532-1535, 2004.

A. M. Brown, A. J. O'Sullivan, and B. D. Gomperts. Induction of exocytosis from permeabilized mast cells by the guanosine triphosphatases Rac and Cdc42. *Mol.Biol.Cell* 9 (5):1053-1063, 1998.

N. D. Burg and M. H. Pillinger. The neutrophil: function and regulation in innate and humoral immunity. *Clin.Immunol.* 99 (1):7-17, 2001.

K. Burridge and K. Wennerberg. Rho and Rac take center stage. *Cell* 116 (2):167-179, 2004.

J. B. Burritt, C. W. Bond, K. W. Doss, and A. J. Jesaitis. Filamentous phage display of oligopeptide libraries. *Anal.Biochem.* 238 (1):1-13, 1996.

E. Caron and A. Hall. Identification of two distinct mechanisms of phagocytosis controlled by different Rho GTPases. *Science* 282 (5394):1717-1721, 1998.

G. Chimini and P. Chavrier. Function of Rho family proteins in actin dynamics during phagocytosis and engulfment. *Nat.Cell Biol.* 2 (10):E191-E196, 2000.

D. Cox, P. Chang, Q. Zhang, P. G. Reddy, G. M. Bokoch, and S. Greenberg. Requirements for both Rac1 and Cdc42 in membrane ruffling and phagocytosis in leukocytes. *J.Exp.Med.* 186 (9):1487-1494, 1997.

P. M. Dang, J. L. Johnson, and B. M. Babior. Binding of nicotinamide adenine dinucleotide phosphate to the tetratricopeptide repeat domains at the N-terminus of p67PHOX, a subunit of the leukocyte nicotinamide adenine dinucleotide phosphate oxidase. *Biochemistry* 39 (11):3069-3075, 2000.

A. K. Das, P. W. Cohen, and D. Barford. The structure of the tetratricopeptide repeats of protein phosphatase 5: implications for TPR-mediated protein-protein interactions. *EMBO J.* 17 (5):1192-1199, 1998.

J. F. Dawson, E. P. Sablin, J. A. Spudich, and R. J. Fletterick. Structure of an F-actin trimer disrupted by gelsolin and implications for the mechanism of severing. *J.Biol.Chem.* 278 (2):1229-1238, 2003.

S. Etienne-Manneville and A. Hall. Rho GTPases in cell biology. *Nature* 420 (6916):629-635, 2002.

M. D. Filippi, C. E. Harris, J. Meller, Y. Gu, Y. Zheng, and D. A. Williams. Localization of Rac2 via the C terminus and aspartic acid 150 specifies superoxide generation, actin polarity and chemotaxis in neutrophils. *Nat.Immunol.* 5 (7):744-751, 2004.

R. Foster, K. Q. Hu, Y. Lu, K. M. Nolan, J. Thissen, and J. Settleman. Identification of a novel human Rho protein with unusual properties: GTPase deficiency and in vivo farnesylation. *Mol.Cell Biol.* 16 (6):2689-2699, 1996.

J. L. Freeman, M. L. Kreck, D. J. Uhlinger, and J. D. Lambeth. Ras effector-homologue region on Rac regulates protein associations in the neutrophil respiratory burst oxidase complex. *Biochemistry* 33 (45):13431-13435, 1994.

Y. Gao, J. B. Dickerson, F. Guo, J. Zheng, and Y. Zheng. Rational design and characterization of a Rac GTPase-specific small molecule inhibitor. *Proc.Natl.Acad.Sci.U.S.A* 101 (20):7618-7623, 2004.

Y. Gu, M. D. Filippi, J. A. Cancelas, J. E. Siefring, E. P. Williams, A. C. Jasti, C. E. Harris, A. W. Lee, R. Prabhakar, S. J. Atkinson, D. J. Kwiatkowski, and D. A. Williams. Hematopoietic cell regulation by Rac1 and Rac2 guanosine triphosphatases. *Science* 302 (5644):445-449, 2003.

J. M. Harlan. Leukocyte adhesion deficiency syndrome: insights into the molecular basis of leukocyte emigration. *Clin.Immunol.Immunopathol.* 67 (3 Pt 2):S16-S24, 1993.

P. A. Janmey and U. Lindberg. Cytoskeletal regulation: rich in lipids. *Nat.Rev.Mol.Cell Biol.* 5 (8):658-666, 2004.

A. J. Jesaitis and R. A. Allen. Activation of the neutrophil respiratory burst by chemoattractants: regulation of the N-formyl peptide receptor in the plasma membrane. *J.Bioenerg.Biomembr.* 20 (6):679-707, 1988.

C. Johnson-Leger and B. A. Imhof. Forging the endothelium during inflammation: pushing at a half-open door? *Cell Tissue Res.* 314 (1):93-105, 2003.

V. L. Katanaev. Signal transduction in neutrophil chemotaxis. *Biochemistry (Mosc.)* 66 (4):351-368, 2001.

V. A. Klenchin, J. S. Allingham, R. King, J. Tanaka, G. Marriott, and I. Rayment. Trisoxazole macrolide toxins mimic the binding of actin-capping proteins to actin. *Nat.Struct.Biol.* 10 (12):1058-1063, 2003.

R. C. Ladner, A. K. Sato, J. Gorzelany, and M. de Souza. Phage display-derived peptides as therapeutic alternatives to antibodies. *Drug Discov.Today* 9 (12):525-529, 2004.

K. Lapouge, S. J. Smith, P. A. Walker, S. J. Gamblin, S. J. Smerdon, and K. Rittinger. Structure of the TPR domain of p67phox in complex with Rac.GTP. *Mol.Cell* 6 (4):899-907, 2000.

W. L. Lee, R. E. Harrison, and S. Grinstein. Phagocytosis by neutrophils. *Microbes.Infect.* 5 (14):1299-1306, 2003.

S. Li, A. Yamauchi, C. C. Marchal, J. K. Molitoris, L. A. Quilliam, and M. C. Dinauer. Chemoattractant-stimulated Rac activation in wild-type and Rac2-deficient murine neutrophils: preferential activation of Rac2 and Rac2 gene dosage effect on neutrophil functions. *J.Immunol.* 169 (9):5043-5051, 2002.

L. M. Machesky and A. Hall. Role of actin polymerization and adhesion to extracellular matrix in Rac- and Rho-induced cytoskeletal reorganization. *J.Cell Biol.* 138 (4):913-926, 1997.

B. M. Mumey, B. W. Bailey, B. Kirkpatrick, A. J. Jesaitis, T. Angel, and E. A. Dratz. A new method for mapping discontinuous antibody epitopes to reveal structural features of proteins. *J.Comput.Biol.* 10 (3-4):555-567, 2003.

J. F. Oram, A. M. Vaughan, and R. Stocker. ATP-binding cassette transporter A1 mediates cellular secretion of alpha-tocopherol. *J.Biol.Chem.* 276 (43):39898-39902, 2001.

S. A. Patat, R. B. Carnegie, C. Kingsbury, P. S. Gross, R. Chapman, and K. L. Schey. Antimicrobial activity of histones from hemocytes of the Pacific white shrimp. *Eur.J.Biochem.* 271 (23-24):4825-4833, 2004.

N. C. Price. Conformational issues in the characterization of proteins. *Biotechnol.Appl.Biochem.* 31 (Pt 1):29-40, 2000.

M. T. Quinn, T. Evans, L. R. Loetterle, A. J. Jesaitis, and G. M. Bokoch. Translocation of Rac correlates with NADPH oxidase activation. Evidence for equimolar translocation of oxidase components. *J.Biol.Chem.* 268 (28):20983-20987, 1993.

A. J. Ridley, H. F. Paterson, C. L. Johnston, D. Diekmann, and A. Hall. The small GTP-binding protein rac regulates growth factor-induced membrane ruffling. *Cell* 70 (3):401-410, 1992.

A. J. Ridley and A. Hall. The small GTP-binding protein rho regulates the assembly of focal adhesions and actin stress fibers in response to growth factors. *Cell* 70 (3):389-399, 1992.

A. W. Roberts, C. Kim, L. Zhen, J. B. Lowe, R. Kapur, B. Petryniak, A. Spaetti, J. D. Pollock, J. B. Borneo, G. B. Bradford, S. J. Atkinson, M. C. Dinauer, and D. A. Williams. Deficiency of the hematopoietic cell-specific Rho family GTPase Rac2 is characterized by abnormalities in neutrophil function and host defense. *Immunity.* 10 (2):183-196, 1999.

D. Roos, R. van Bruggen, and C. Meischl. Oxidative killing of microbes by neutrophils. *Microbes.Infect.* 5 (14):1307-1315, 2003.

A. Schmidt and M. N. Hall. Signaling to the actin cytoskeleton. *Annu.Rev.Cell Dev.Biol.* 14:305-38.:305-338, 1998.

A. A. Schmitz, E. E. Govek, B. Bottner, and L. Van Aelst. Rho GTPases: signaling, migration, and invasion. *Exp.Cell Res.* 261 (1):1-12, 2000.

T. Schwede, A. Diemand, N. Guex, and M. C. Peitsch. Protein structure computing in the genomic era. *Res.Microbiol.* 151 (2):107-112, 2000.

S. S. Sidhu. Phage display in pharmaceutical biotechnology. *Curr.Opin.Biotechnol.* 11 (6):610-616, 2000.

S. S. Sidhu, W. J. Fairbrother, and K. Deshayes. Exploring protein-protein interactions with phage display. *Chembiochem.* 4 (1):14-25, 2003.

J. A. Smith. Neutrophils, host defense, and inflammation: a double-edged sword. *J.Leukoc.Biol.* 56 (6):672-686, 1994.

D. Sorescu, D. Weiss, B. Lassegue, R. E. Clempus, K. Szocs, G. P. Sorescu, L. Valppu, M. T. Quinn, J. D. Lambeth, J. D. Vega, W. R. Taylor, and K. K. Griendling. Superoxide production and expression of nox family proteins in human atherosclerosis. *Circulation* 105 (12):1429-1435, 2002.

C. X. Sun, G. P. Downey, F. Zhu, A. L. Koh, H. Thang, and M. Glogauer. Rac1 is the small GTPase responsible for regulating the neutrophil chemotaxis compass. *Blood* 104 (12):3758-3765, 2004.

R. M. Taylor, J. B. Burritt, D. Baniulis, T. R. Foubert, C. I. Lord, M. C. Dinauer, C. A. Parkos, and A. J. Jesaitis. Site-specific inhibitors of NADPH oxidase activity and structural probes of flavocytochrome b: characterization of six monoclonal antibodies to the p22phox subunit. *J.Immunol.* 173 (12):7349-7357, 2004.

M. Torti, A. Bertoni, I. Canobbio, F. Sinigaglia, E. G. Lapetina, and C. Balduini. Interaction of the low-molecular-weight GTP-binding protein rap2 with the platelet cytoskeleton is mediated by direct binding to the actin filaments. *J.Cell Biochem.* 75 (4):675-685, 1999.

P. J. Van Haastert and P. N. Devreotes. Chemotaxis: signalling the way forward. *Nat.Rev.Mol.Cell Biol.* 5 (8):626-634, 2004.

P. V. Vignais. The superoxide-generating NADPH oxidase: structural aspects and activation mechanism. *Cell Mol.Life Sci.* 59 (9):1428-1459, 2002.

H. C. Welch, W. J. Coadwell, C. D. Ellson, G. J. Ferguson, S. R. Andrews, H. Erdjument-Bromage, P. Tempst, P. T. Hawkins, and L. R. Stephens. P-Rex1, a PtdIns(3,4,5)P3- and Gbetagamma-regulated guanine-nucleotide exchange factor for Rac. *Cell* 108 (6):809-821, 2002.

H. C. Welch, W. J. Coadwell, L. R. Stephens, and P. T. Hawkins. Phosphoinositide 3-kinase-dependent activation of Rac. *FEBS Lett.* 546 (1):93-97, 2003.

E. Werner. GTPases and reactive oxygen species: switches for killing and signaling. *J.Cell Sci.* 117 (Pt 2):143-153, 2004.

B. Wojciak-Stothard, S. Potempa, T. Eichholtz, and A. J. Ridley. Rho and Rac but not Cdc42 regulate endothelial cell permeability. *J.Cell Sci.* 114 (Pt 7):1343-1355, 2001.

D. K. Worthylake, K. L. Rossman, and J. Sondek. Crystal structure of Rac1 in complex with the guanine nucleotide exchange region of Tiam1. *Nature* 408 (6813):682-688, 2000.

R. A. Worthylake, S. Lemoine, J. M. Watson, and K. Burridge. RhoA is required for monocyte tail retraction during transendothelial migration. *J.Cell Biol.* 154 (1):147-160, 2001.

R. A. Worthylake and K. Burridge. Leukocyte transendothelial migration: orchestrating the underlying molecular machinery. *Curr.Opin.Cell Biol.* 13 (5):569-577, 2001.

Q. Yan, E. Cho, S. Lockett, and K. Muegge. Association of Lsh, a regulator of DNA methylation, with pericentromeric heterochromatin is dependent on intact heterochromatin. *Mol.Cell Biol.* 23 (23):8416-8428,